EPSC2018

EXO2 abstracts

13 Sep 2018 15:37:04

EPSC Abstracts
Vol. 12, EPSC2018-12, 2018
European Planetary Science Congress 2018

Condensation of gas-dust particles in the dust shells of protostars and the formation of "embryos" of planets

T. Abdulmyanov
Kazan State Power Engineering University, Kazan, Russia (abdulmyanov.tagir@yandex.ru / Fax: +7-843-5624356)

Abstract

The paper analyzes the basic ideas of migration of primary solids in passive and active protoplanetary disks. Comparing the "hybrid" migration models [2] with the Safronov model, it is noted that the hypothesis of fast migration of "embryos" contradicts the basic laws of celestial mechanics and Laplace's stability theorem. Using the model of wave perturbations of dust shells of protostars and the model of orbital resonance, a general model for the formation of "embryos" of planets has been constructed. The appearance of a single "embryo" in protoplanetary rings is explained by the effect of the 1/1 orbital resonance mechanism.

1. Introduction

According to the results of studies, the migration and growth of "embryos" of planets in passive discs can occur through the internal and external trajectories of the Lindblad resonance, as well as through the librational trajectories of orbital resonance. It is also shown that in the centers of turbulent motion of particles in active disks, initial formation and growth of the "embryos" of the planets is possible. At the same time, questions remain to "hybrid" hypotheses [2], in which a rapid migration of the "embryos" of planets from the giant planet zone to the zone of planets of the terrestrial group is expected. Such migration is contrary to the basic laws of celestial mechanics and the Laplace stability theorem. In this paper, the main arguments of "hybrid" hypotheses are analyzed and the mechanism of equilibrium of the dust shells of the protostar is considered, with the help of which an attempt is made to explain the formation and growth of "embryos" of planets without the condition of their rapid migration. Using the model of wave perturbations of the dust shells of protostars and the orbital resonance model [1], a general model for the formation of "embryos" of planets has been constructed, starting with the primary condensation of gas-dust particles in dust shells, before the formation and growth of "embryos" of planets on the equatorial plane of protostars.

2. Growth of sizes and masses of small particles

Causes that can interfere with gravitational instability can be enclosed in the general mechanism of star formation, part of which is the formation of a protoplanetary disk. Connection with gravitational compression of protostars, it is possible to change the regime of unstable equilibrium of the dust shells to a stable equilibrium. The stable equilibrium of the dust shells is established when the following condition is fulfilled: $4\pi G\rho_0 / c^2 - \lambda_k^2 / R_0^2 + \gamma^2 > 0,$ (1)

where ρ_0 is the average density of the protostar of radius R_0, $\gamma = [1/(z_1 - z_0)] \cdot ln\,(\rho(z_0)/\rho(z_1))$}, z_0, z_1 is the initial and final radius of the protostar, λ_k are the zeros of the Bessel function $J_0(r)$, G is the gravitational constant, and c is the speed of sound for the dust shells. Fig. 1a is shown the form of the density waves corresponding to the stable equilibrium condition (1). Periodic displacements of the maxima could redistribute dust particles even in the dust shells so that the settling solid particles formed dense protoplanetary rings located at a distance d ($d = 2R_0$, $R_0 = 5$ AU, Fig. 1a) from each other. According to model of wave fragmentation, protoplanetary rings of planets more distant from the center of the protostar will be formed first, and then those that are located closer to the center. It follows there is no need to explain the reasons for the migration of "embryos" of planets from the zone of giant planets into the zone of planets of the terrestrial group. The influx of dense particles for the rapid growth of the "embryos" of the planets will be provided by the wave mechanism, the rapid settling of the solid particles of the dust shells on the equatorial plane, and the wave fragmentation of the dust shells, including in the equatorial plane where the protoplanetary disk is formed.

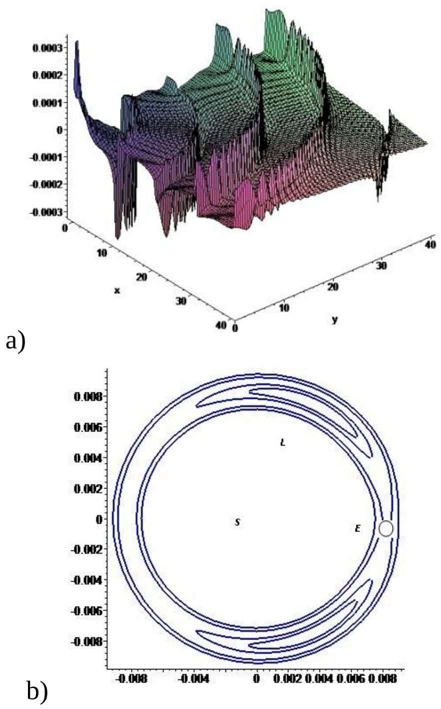

Figure 1: (a) 3-*D* density profiles $\rho_1(r, \varphi, t)$ for t = 0. (b) Libration orbits of small celestial bodies near the orbital resonance 1/1 for resonance parameters α^2 = 0.6; 0.8; 1.7; 2.2 and inclination of the orbits i = 25°, $r^* = r$ - 0.817 (projections onto the plane of Jupiter's orbit).

Unlike the Safronov model [3], the accretion of small bodies into the "embryos" of planets occurs through the librational orbits of the 1/1 resonance. In such a model, the "embryos" will be formed [1] on one of the vertices of an equilateral triangle *SLE*, where *S* is the center of the protostar, *L* is one of the two triangular points of Lagrange L_4 and L_5, and *E* is the "embryo" (Fig 1b). In accordance with the barometric formula [3], in the absence of turbulence, solid particles will settle in a short time to the equatorial plane, forming a layer of increased density in it. At critical values of disk density, bodies of kilometer sizes will arise [3]. Modern ideas about the gravitational contraction of protostars are based on the model of Shakura and Syunyaev [4]. In the model of Shakura and Syunyaev, only the scenario of gravitational compression of protostars is considered and the possibility of temporary equilibrium is not considered. However, considering the complexity of the trajectories of entering the Main sequence of stars comparable in mass to the mass of the Sun, this possibility should be considered.

3. Wave model of fragmentation of dust shells

The gravitational instability of the protoplanetary disk in the zone of formation of the Earth group planets could have come due to the inflow of settling dense particles that originate in the fragmentation of the dust envelopes of young stars. In view of the fact that the model of wave fragmentation essentially and fundamentally differs from the migration growth model of the "embryos" of the terrestrial planets [2], we list all the main stages of the formation of "embryos" of planets in the wave model: 1) A gas dust cloud whose mass is equal to the mass of the Sun *Ms* will be gravitationally unstable if it has a radius of 2×10^6 *Rs*, an average density $\rho_0 = 10^{-19}$ g/cm^3, the temperature T = 15*K* and will be compressed. 2) According to the model of wave fragmentation, under the conditions of stable equilibrium (1), the mechanism of density waves, which will form solid particles, will act in the dust shells. As they form, these particles will settle on the equatorial plane. As a result of the action of density waves, the zones of the dust envelope removed at a distance of $2R_0$ will be stripped. The same distances will be between protoplanetary rings formed as a result of the settling of solid particles. 3) In accordance with the model considered here, the protoplanetary rings of Pluto, Neptune, Uranus and Saturn began to form substantially earlier than the rings of other planets. The Neptune ring was formed at the beginning of the Hayashi stage (4.5836 billion years ago). After this, after 2.0186 million years and 2.3857 million years, the rings of Uranus and Pluto began to form.

4. Summary and Conclusions

According to the wave model of the fragmentation of the dust shells of protostars, the essential difference in the structures of the two groups of planets, giant planets and terrestrial planets can be explained by the fact that these groups of planets formed at different stages of protostar compression. These stages corresponded to essentially different parameters ($d = 2R_0$) of the wave mechanism, which acted in the dust envelope of the protostar.

References

[1] Abdulmyanov T.R. //Moscow Univ. Phys. Bull. 2014, **69**, 558.
[2] Nayakshin S. //Mon. Not. R. Astron. Soc. 2014, **441**, 1380.
[3] Safronov, V. S.: Evolution of the proto-planetary cloud and formation of the Earth and other planets, NASA TTF-677, 1972.
[4] Shakura N.I., Sunyaev R.A. // A&A, 1973, **24**, 337.

EPSC Abstracts
Vol. 12, EPSC2018-13, 2018
European Planetary Science Congress 2018

The First Accurate and Quantitative Model of the Formation of Terrestrial Planets and Origin of Earth's Water

Nader Haghighipour(1) and Thomas Maindl(2)
(1) Institute for Astronomy, University of Hawaii, USA, (2) Dept. Astrophysics, Univ. Vienna, Austria (nader@ifa.hawaii.edu)

Abstract

We have developed a comprehensive methodology to model the formation of terrestrial planets and origin of Earth's water. Using a combination of SPH and N-body codes, we model the collisions and growth of embryos to planetary bodies accurately. We simulate collisions directly, and for the first time, consider the loss of water due to the heat of the impact, mass-removal during collisions, and ice-sublimation during orbital evolution of bodies. Our results present a more accurate and quantifiable estimate of the water delivered to Earth and are informed directly from geological evidence of Earth evolution. Our methodology also tracks the transfer of water and volatiles from one body to another, self-consistently.

1. Introduction

It is widely accepted that collisions among solid bodies, ignited by their interactions with planetary embryos is key to the formation of terrestrial planets and transport of water and other volatiles to their accretion zones. Unfortunately, due to computational limitations, these collisions are often treated in a rudimentary way where impacts are considered to be perfectly inelastic and water is fully transferred from one object to the other. This perfect-merging assumption, while useful for the proof of the concept, portrays an unrealistic image of the formation and properties of the final planetary bodies that is unquantifiable and grossly overestimates the masses of these objects and the amount of their volatiles. It also entirely neglects collisional-loss of volatiles and draws an unrealistic connection between these properties and the chemical structure of the protoplanetary disk. Modern collision models have tried to overcome these difficulties by determining the outcome of collisions and the number of produced fragments by either using an impact catalog or a pre-set prescription. However, these models still do not treat the transport and transfer of water accurately. They consider no loss of water during the orbital evolution of an object and consider perfect transfer of volatiles from one body to the other after a collision.

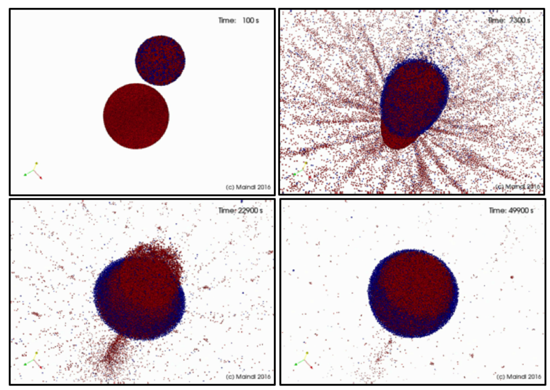

Figure 1: Snapshots of the SPH simulation of an impact between a 0.8 Moon-sized embryo with 10% water and a dry, 0.5 Mars-sized object (impact velocity = 6 km/s).

We have developed a new and comprehensive approach in simulating collisions and the growth of embryos to planetary bodies where we use a combination of SPH and N-body codes to model collisions as well as the transport/transfer of chemical compounds accurately. We simulate collisions directly (i.e., without using impact catalogues and fragmentation prescriptions), and for the first time, consider the loss of water due to the heat of the impact, mass-removal during collisions, and ice-sublimation during orbital evolution of bodies.

2. Description of our codes

We simulate terrestrial planet formation using a combined N-body+SPH code. Our N-body code has been developed to allow collisions to happen only when bodies are physically in contact with one another. At that stage, we model the collision using our full 3D SPH impact code [2,3].

Our SPH code includes material strength and self-gravity, and implements full elastoplastic continuum mechanics extended by a model for simulating brittle failure [4, 5]. It also includes a fragmentation prescription and accounts for evaporation during the impact as well as the re-accretion of scattered materials. Following [6], we apply a tensorial correction to achieve first-order consistency. The material model is based on the Tillotson equation of state [7]. As a result of this approach, i.e., SPH modeling of collisions within the N-body integration, our simulations are free of collisional artifacts and present more accurate values for the mass and volatile contents of the final planets.

3. Simulations and Results

To accurately model the formation of terrestrial planets and the delivery of water, we carried out a large number of traditional N-body simulations. Each simulation included a few hundred Moon- to Mars-sized planetary embryos and several thousand km-sized planetesimals. To avoid un-necessary computations, we limited SPH simulations to only collisions with the seed embryos that resulted in the formation of final planetary bodies. For each seed embryo, we simulated its collision with other embryos as well as planetesimals. The latter is necessary to account for the loss of water due to ice sublimation from impact craters. In each simulation, we determined the amount of ice exposed at the bottom and walls of the crater as well as those re-accreted on the surface of the embryo. We then calculated the amount of sublimated ice until that embryo collided with another embryo or the exposed ice was fully sublimated.

Each collision of a seed embryo with other protoplanetary bodies was simulated using our SPH code. We considered embryos to be rocky and used the parameters for rock (basalt) and water ice as stated in [3]. Porosity was included using the $P-\alpha$ model [8-11]. At the lowest resolution, each embryo was resolved to at least 500,000 SPH particles. We determined the water content of the resulting body by keeping track of each SPH particle, and continued this process for subsequent collisions until the last impact event when the final planetary body formed. During this process, mass of the final planet and its water content were accurately determined. Figure 1 shows a snapshot of a sample of our embryo-embryo SPH simulations.

We carried out 60 SPH simulations of collisions between embryos of Ceres size and larger. Results indicated that even for collisions at moderate velocities, the amount of water lost during the impact is

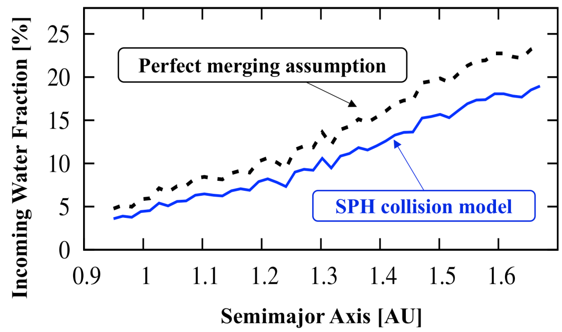

Figure 2: A comparison between the amount of water introduced to the terrestrial region in perfect merging and in our model.

non-negligible. For instance, for embryos colliding at twice their mutual escape velocity, 10% to 60% of their water is lost in a collision. Figure 2 shows this in more detail. Noting that in addition to collision, water is also lost due to evaporation and sublimation, and a seed embryo may be subject to a large number of collisions until a planetary body is formed, the above-mentioned water-loss percentages may be even larger.

4. Summary and Conclusions

Accurate simulations of collisions of protoplanetary bodies show that tradition-al N-body modeling of terrestrial planet formation overestimates the amount of the mass and water content of the final planets by over 60%. This implies that, as indicated by [1], i) small planets such as Mars can also form in these simulations when collisions are treated properly and ii) the distribution of water, volatiles, and chemical compounds cannot be post-formation and must be handled during a simulation, through proper treatment of collisions.

5. References

[1] Haghighipour, N. & Winter, O. C. (2016) CMDyA, 124, 235. [2] Maindl, T. I., et al (2013) Astron. Nachr., 334, 996. [3] Schäfer, C., et al (2016) A&A, 590, A19. [4] Benz, W. & Asphaug, E. (1994) Icarus, 107, 98. [5] Benz, W. & Asphaug, E. (1995) CPC, 87, 253. [6] Schäfer, C. et al (2007) A&A, 470, 733. [7] Tillotson, J. H. (1962) GA-3216, General Dynamics. [8] Hermann, W. (1969) J. Appl. Phys., 40, 2490. [9] Carroll, M. M. & Holt, A. C. (1972) J. Appl. Phys., 43, 1626. [10] Jutzi, M., et al (2008), Icarus, 198, 242. [11] Jutzi, M., et al (2009) Icarus, 201, 802.

EPSC Abstracts
Vol. 12, EPSC2018-32, 2018
European Planetary Science Congress 2018

One step closer to unveiling the planetesimal-formation process

Jürgen Blum
Institut für Geophysik und extraterrestrische Physik, TU Braunschweig, Germany (j.blum@tu-bs.de)

Abstract

The formation of planetesimals has successfully been modelled by consecutive sticking collisions all the way from µm-sized dust to km-sized bodies as well as by first forming mm-sized dust aggregates which then undergo hydrodynamic spatial concentration until their collective gravitational attraction results in a gentle collapse to multi-km-sized objects. With more and more empirical evidence emerging from laboratory measurements, numerical modelling and observations, the two-stage scenario now seems to be the most likely. Here I will show the evidence that speaks in favour of a gravitational-collapse model.

1. The two competing models of planetesimal formation

It is undisputed that planetesimal formation in protoplanetary discs (PPDs) starts with (sub-)µm-sized solid grains of dust (metals, oxides, silicates, organic materials, depending on the ambient temperature) and/or ice (H_2O, CO_2, CO, NH_3, CH_4). These grains experience mutual collisions, which initially are so gentle that they always result in the sticking of the grains and, thus, lead to the formation of aggregates. With increasing aggregate size (assuming a fractal dimension of the aggregates >2), the collision velocities systematically increase. At some point, the collision speed exceeds the sticking threshold of the aggregates, whereupon the initial growth stage ends (see Ref. [1] for a recent review about the dust-aggregate collision model). Depending on the PPD model and the grain properties (particle size and material), the final aggregate size is in the range ~0.1-10 mm [5,3]. This first growth stage is common for the two competing planetesimal-formation models, which will be presented hereafter. Details and references about the models, including benefits and problems as well as the properties of the resulting planetesimals, can also be found in Ref. [1].

1.1 The collisional-growth model

Laboratory experiments have shown that for collision velocities exceeding the fragmentation threshold of the smaller of the two colliding dust aggregates, growth of the larger aggregate by mass transfer from the fragmenting aggregate can occur. Although the growth rate of this process is relatively small, it can in principle ultimately lead to the formation of bodies with sizes on the order of 1 km.

1.2 The gravitational-collapse model

If sedimentation towards the PPD mid-plane or hydrodynamic processes can locally concentrate the typically mm- to cm-sized aggregates (“pebbles”) resulting from the first growth stage, the streaming instability is capable of further concentration until a gentle gravitational collapse occurs. The resulting planetesimals are typically 100 km in size (with a power-law size distribution) and the required timescales are much shorter than for the collisional-growth model.

2. Planetesimal properties and empirical evidence from cometary nuclei

Due to the different physical process eventually leading to planetesimals in the two models described in Sect. 1, their properties differ considerably, which provides the opportunity for empirical tests with planetesimals in the Solar System (see Ref. [1] for details).

2.1 Properties of planetesimals formed by the collisional-growth model

Due to the high collision velocities in the mass-transfer regime (typically 50 m s^{-1}), the growing planetesimals possess a porosity of only ~60%, a tensile strength of ~10^3-10^4 Pa, and no characteristic particle size between the dust grains (~1 µm) and the planetesimal size (~1 km).

2.2 Properties of planetesimals formed by the gravitational-collapse model

Depending on the size of the final planetesimal, the "pebbles" from the gravitationally collapsing cloud either survive intact (size $\lesssim$ 10-50 km) or are being crushed during the collapse or hydrostatically inside the planetesimal (size $\gtrsim$ 10-50 km). In the latter case, the planetesimal properties are comparable to those of the bodies formed by collisional growth, except for the final planetesimal size. However, for small planetesimals, a porosity of ~70-80%, a tensile strength of ~1-10 Pa, and the occurrence of a characteristic size scale between the dust grains (~1 µm) and the planetesimal size (~1-10 km), namely the "pebble" size of ~1-10 mm is expected.

2.3 Cometary nuclei as evidence for planetesimal formation by a gravitational collapse of a "pebble" cloud

Cometary nuclei, with typical sizes of 1-10 km are the ideal objects to search for empirical evidence about their formation, because they are small enough to preserve dust "pebbles" if they were formed by the gravitational collapse and they experienced at most sub-catastrophic collisions, which kept major parts of the original planetesimal matter structurally intact [4].

With recent advances in investigations of comets, the following evidences have been collected in favour of the gravitational-collapse model (see Ref. [1] and references therein for more details):

- The presence of fractal particles in the coma of comet 67P, as found by the Rosetta mission, can only be explained if these aggregates were remnants from the solar nebula and were safely stored in between cm-sized denser entities, the "pebbles" [2]. The fractal particles bear evidence that comets are very primitive and contain (fractal and non-fractal) dust aggregates from the formation era of the Solar System.
- With the Rosetta/Philae spacecraft having visited comet 67P, it is very likely that the overall porosity of the nucleus is between 69% and 75% (depending on the composition of the comet) and that the tensile strength is in the range 1-10 Pa. These values match the predictions by the gravitational-collapse model.
- The dust activity of comets is caused by the outgassing of volatile species, primarily of water ice. Thermal models of the sub-surface regions of comets when they approach the Sun make predictions about the ice temperature under the desiccated dust layer. Converting this temperature into an outgassing rate and a local gas pressure shows that it is very unlikely that this pressure ever exceeds ~1 Pa. Thus, in order to overcome the cohesion of the dust layer above the ice, its tensile strength must be accordingly small. The gravitational collapse model inherently predicts this for aggregate sizes of ~1 cm or above. In fact, most of the dust mass released by comets is in particles of typically this size (or larger).

Acknowledgements

I thank the Deutsche Forschungsgemeinschaft (DFG) and the Deutsches Zentrum für Luft- und Raumfahrt (DLR) for continuous support.

References

[1] Blum, J.: Dust evolution in protoplanetary discs and the formation of planetesimals – What have we learned from laboratory experiments? Space Science Reviews, Vol. 214, 52, 2018.

[2] Fulle, M. and Blum, J.: Fractal dust constrains the collisional history of comets, Monthly Notices of the Royal Astronomical Society, Vol. 469, pp. S39-S44, 2017.

[3] Lorek, S., Lacerda, P., and Blum, J.: Local growth of dust- and ice-mixed aggregates as cometary building blocks in the solar nebula, Astronomy & Astrophysics, Vol. 611, A18, 2018.

[4] Schwartz, S., Michel, P., Jutzi, M., Marchi, S., Zhang, Y., and Richardson, D.: Catastrophic disruptions as the origin of bilobate comets, Nature Astronomy, Advanced Online Publication, 2018.

[5] Zsom, A. Ormel, C., Güttler, C., Blum, J., and Dullemond, C.: The outcome of protoplanetary dust growth: pebbles, boulders, or planetesimals? II. Introducing the bouncing barrier, Astronomy & Astrophysics, Vol. 513, A57, 2010.

EPSC Abstracts
Vol. 12, EPSC2018-59, 2018
European Planetary Science Congress 2018

Metalicity effect and planet mass function in pebble-based planet formation models

Natacha Brügger (1), Yann Alibert (1), Sareh Ataiee (2), Willy Benz (1)
(1) Physikalisches Institut & Center for Space and Habitability, Universität Bern, CH-3012 Bern, Switzerland, (2) Institut für Astronomie & Astrophysik, Universität Tübingen, Tübingen, Germany

Abstract

Adopting the Bitsch et al. 2015 disc model we use a population synthesis approach to compare the formed planets with observations. We find that keeping the same parameters as in Bitsch et al. 2015 leads to no planet growth. Indeed a large fraction of the heavy elements should be put into pebbles in order to form massive planets using this approach. The resulting mass functions show a huge amount of giants and a lack of Neptune mass planets, which are abundant according to observations. To overcome this issue we include the computation of the internal structure for the planetary atmosphere to our model. This leads to the formation of Neptune mass planets but no observable giants. Reducing the opacity of the planetary envelope finally matches observations better. Using this model we observe a metalicity impact.

1. Introduction

One of the main scenarios of planet formation is the core accretion model where first a massive core forms accreting solids, either planetesimals or pebbles, and then accretes a gaseous envelope. Classical planetesimal accretion scenario predicts that the time needed to form a giant planet's core is much longer than expected disc lifetimes. This leads to the development of another scenario, in which cores grow by accreting pebbles, which are much smaller and thus more easily trapped by the planets gravity before being accreted, leading to more rapid formation of the core.

2. Bitsch et al. 2015 model

We initially use the disc model given by Bitsch et al. 2015 (B15). To test our implementation we aimed to reproduce their results and, getting encouraging results by recreating their gas disc model, we compared the planet growth (Fig. 1). The outcomes are completely different: no planets grow. The issue comes from the computation of the pebble flux , which should be evaluated at the pebble growth radius r_g and not at the location of the planet:

$$\dot{M}_{\rm pebbles}(r) = 2\pi r_{\rm g} \frac{dr_{\rm g}}{dt} Z_{\rm peb}(r_{\rm g}) \Sigma_{\rm gas}(r_{\rm g}) \qquad (1)$$

Applying the wrong flux equation (taking $\Sigma_{\rm gas}(r)$ instead of $\Sigma_{\rm gas}(r_{\rm g})$) in our model allows us to reproduce B15 results (the thin and thick lines in Fig. 1 overlap).

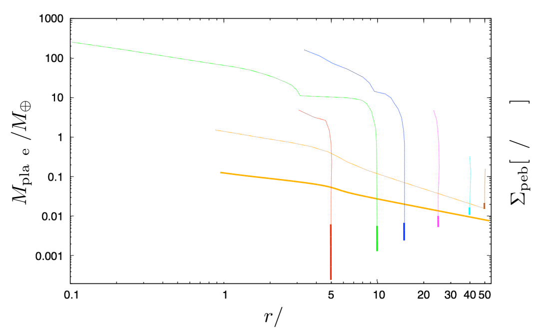

Figure 1: Planet growth comparison for the results of B15 (thin lines) and our results (thick lines).

3. Increasing the amount of pebbles

With a view of forming planets and using the correct equation for the flux of pebbles, we increase the amount of solids that form pebbles. We decide to put 90% of the total amount of solids into pebbles and 10% into dust. This ratio allows the formation of giant planets and prevent the migration from being too efficient. However, comparison with observations shows a lack of Neptune mass planets.

4. Solving the internal structure of the planet

In the B15 model the internal structure is very simple: once the planet has reached the pebble isolation mass, a rapid gas accretion phase starts. In reality, if the isolation mass is small, once it is reached, the envelope contracts. We thus compute the internal structure of the planet. The resulting mass function yields a significant amount of Neptune mass planets, in agreement with observations, but also a total absence of giant planets.

5. Decreasing opacity

An alternative to form giants is the reduction of the opacity of the planet's atmosphere. There are observational hints that this opacity is much smaller than the full interstellar one (Mordasini et al. 2014), which is used in our nominal case. We therefore apply a reduction factor ($f_{\rm opa} = 0.01$). Figure 2 gives the mass functions of the formed planets using the full interstellar opacity and the reduced one. Applying a detection probability given by Mayor et al. 2011 we see that the fraction of planets with masses higher than 20 $M_\oplus$ is significant and a high amount of giant planets are observable.

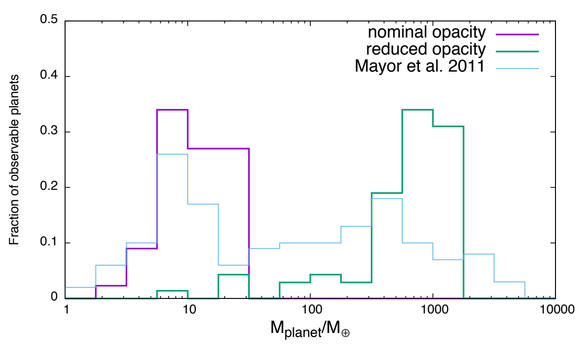

Figure 2: Fraction of observable planets solving the internal structure and using a reduced opacity.

6. Metallicity effect

We then discuss the well established metallicity effect for our internal structure model with a reduced opacity. We see in Fig. 3 that the amount of giant planets increases with metallicity. For metallicities up to $[\mathrm{Fe/H}] = 0, 3$, no planet is observable. Comparing the red and blue curves, we see that a fraction of formed planets (red curve) may be lost in the star (difference between red and blue).

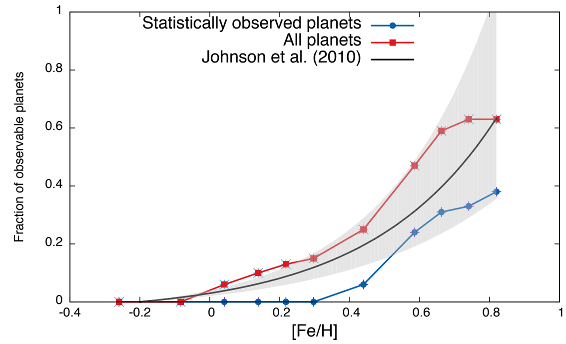

Figure 3: Fraction of planets with radial velocity higher than 20 m/s as a function of the metallicity.

7. Summary and Conclusions

Using the B15 model, the amount of pebbles in the disc should be increased in order to form planets. This model forms mainly giant planets and no Neptune-mass planets. Solving the internal structure equations settles the lack of Neptunes but no giants are created anymore. By reducing the opacity in the model solving the internal structure equations it favours the formation of planets with masses above 20 $M_\oplus$ as well as giant planets. We thus use this last model to discuss the metallicity effect and show that the amount of giant planets increases with the metallicity.

Acknowledgements

This work has been carried out within the frame of the National Centre for Competence in Research PlanetS supported by the Swiss National Science Foundation. The authors acknowledge the financial support of the SNSF.

References

[1] Bitsch, B., Lambrechts, M. & Johansen, A., 2015b, 582, 112

[2] Brügger et al., submitted

[3] Mayor et al. 2011, Astronomy & Astrophysics

[4] Mordasini et al. 2014, Astronomy & Astrophysics 566

EPSC Abstracts
Vol. 12, EPSC2018-132, 2018
European Planetary Science Congress 2018

Gradual desiccation of rocky protoplanets from ^{26}Al-heating

Tim Lichtenberg (1), Gregor J. Golabek (2), Remo Burn (3), Michael R. Meyer (4), Yann Alibert (3,5), Taras V. Gerya (1), Christoph A. Mordasini (3,5)
(1) Institute of Geophysics, ETH Zürich, Switzerland (tim.lichtenberg@phys.ethz.ch), (2) Bayerisches Geoinstitut, University of Bayreuth, Germany, (3) Physikalisches Institut, University of Bern, Switzerland, (4) Department of Astronomy, University of Michigan, United States, (5) Center for Space and Habitability, University of Bern, Switzerland

Abstract

The formation and distribution of Earth-like planets remains poorly constrained. However, stochasticity during accretion and the variety of exoplanet compositions favor rocky worlds covered in thick volatile ice layers as the dominant family of terrestrial analogues [1], deviating from the water-poor inner-Solar system planets. Here, we demonstrate the power of ^{26}Al, a short-lived radioisotope abundant in the early Solar system, to control the water content of terrestrial exoplanets. Using numerical models of planet formation, evolution, and interior structure [2], we generate synthetic planet populations that are subject to a varying degree of ^{26}Al-heating during accretion [3]. We show that planet bulk water fraction and radius are anti-correlated with the host system's ^{26}Al levels (Fig. 1). This yields a system-wide correlation [4] of bulk abundances, and is consistent with the location-independent scarcity of water within the TRAPPIST-1 planets [5]. The generic sensitivity of exoplanet observables on primordial ^{26}Al inferred from our models suggests two distinct classes of rocky exoplanets: high-^{26}Al systems form small, water-depleted planets, those devoid of ^{26}Al form ocean worlds, with the mean planet radii deviating by up to ~10%.

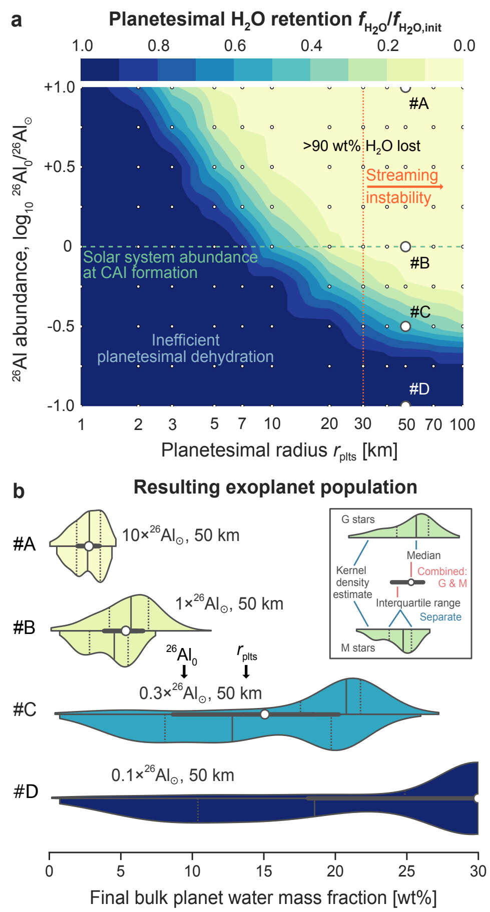

Figure 1: (a) Water retention in planetesimals subject to a varying degree of ^{26}Al heating. (b) Bulk planet water abundances f_{H_2O} in exoplanet populations with M_{planet} = 0.1–10 M_{Earth} and $f_{H_2O} > 0$, formed with fixed ^{26}Al$_0$ and planetesimal radius r_{plts}.

References

[1] Leger, A. et al.: Icarus 169, 499–504 (2004).

[2] Benz, W., Ida, S., Alibert, Y., Lin, D. N. C., Mordasini, C.: Protostars and Planets VI, 697–713 (2014).

[3] Lichtenberg, T., Parker, R. J., Meyer, M. R.: Mon. Not. R. Astron. Soc. 462, 3979–3992 (2016).

[4] Millholland, S., Wang, S., Laughlin, G.: Astrophys. J. Lett. 849, L33 (2017).

[5] Grimm, S. L. et al.: Astron. Astrophys., in press, arXiv:1802.01377 (2018).

EPSC Abstracts
Vol. 12, EPSC2018-231, 2018
European Planetary Science Congress 2018

On the stability of 3D exoplanetary systems

Mara Volpi, Anne-Sophie Libert, Arnaud Roisin
naXys, Department of Mathematics, University of Namur, 8 Rempart de la Vierge, 5000 Namur, Belgium
(mara.volpi@unamur.be)

Abstract

To date, more than 600 multiple planet systems have been discovered. Due to the limitations of the detection methods, our knowledge of the extrasolar systems is usually far from complete. In particular, for planetary systems discovered with the radial velocity technique, the inclinations of the orbital planes (and thus their mutual inclination and the planetary masses) are unknown. Our work aims to constrain the observations of several non-resonant two-planet extrasolar systems. Through analytical analysis based on a first-order secular Hamiltonian expansion and numerical explorations performed with a chaos detector, we identify ranges of values for the mutual inclinations which ensure the long-term stability of the detected systems. Particular attention is also given to determine the possibility for the planetary systems to be in a Lidov-Kozai resonant state.

1 Introduction

For two-planet systems detected with the radial velocity method, no information can currently be derived on the mutual inclination between the two orbital planes. For highly inclined systems, Lidov-Kozai resonance ([6, 2]) offers a secular phase-protection mechanism, ensuring the long-term stability of the systems. In particular, [4] have shown that several extrasolar systems have orbital parameters compatible with a Lidov-Kozai resonant state at high mutual inclination. Here, we aim to pursue this study by investigating the spatial architecture of 16 detected planetary systems, focusing in particular on the extent of the resonant region and its consequences on the system stability.

2 Analytical model

We consider the three-body problem of two planets revolving around a central star. To reduce the number of parameters to be considered (each planet has 6 orbital elements), we adopt an analytical approach which allows to reduce the problem to two degrees of freedom. To do so, we refer the orbits to the invariant Laplace plane (as a result of the conservation of the total angular momentum $\mathbf{C}$). Following [5], we expand the Hamiltonian in planar Poincaré variables $(\boldsymbol{\Lambda}, \boldsymbol{\lambda}, \boldsymbol{\xi}, \boldsymbol{\eta})$ and in the parameter $D_2 = ((\Lambda_1 + \Lambda_2)^2 - C^2)/\Lambda_1\Lambda_2$ (as defined in [7]). Being interested in the secular evolution of the system, we average over the fast angles, obtaining the following two degrees of freedom formulation

$$H(D_2, \boldsymbol{\xi}, \boldsymbol{\eta}) = \sum_{j=0}^{ORDECC/2} C_{j,\boldsymbol{m},\boldsymbol{n}}\, D_2^j \sum_{|\boldsymbol{m}|+|\boldsymbol{n}|=0}^{ORDECC-j} \boldsymbol{\xi}^{\boldsymbol{m}} \boldsymbol{\eta}^{\boldsymbol{n}}\,,$$

where *ORDECC* is the maximal order in the eccentricities (here fixed at 12). As shown in previous works (see for instance [3]), if the system is far from a mean-motion resonance, this secular approximation at first order in the masses is accurate enough to describe its evolution. Moreover, for most of the systems, we show that this expansion is valid up to very high values of the mutual inclination ($i_{mut} \simeq 80°$).

3. Parametric study and results

We study the spatial resolution of several extrasolar systems (HD 11506, HD 117618, HD 12661, HD 134987, HD 142, HD 154857, HD 1605, HD 163607, HD 164922, HD 169830, HD 177830, HD 207832, HD 37605, HD 4732, HD 74156 and HD 85390), by varying the mutual inclination i_{mut} and the inclination of the orbital planes. We choose to vary both orbital plane inclinations in the same way (parameter i), to keep the mass ratio constant. The other orbital elements of the systems are taken from the online database `exoplanets.eu`.

For each system, we provide ranges of values of i_{mut} and i which ensure the long-term stability of the system. On the one hand, we identify precisely the extent of the Lidov-Kozai region characterised by the libration of the argument of the pericenter of the inner planet ω_1. On the other hand, regular 3D planetary configurations are revealed by means of the MEGNO chaos indicator [1]. An example is shown in Fig. 1 for HD 11506.

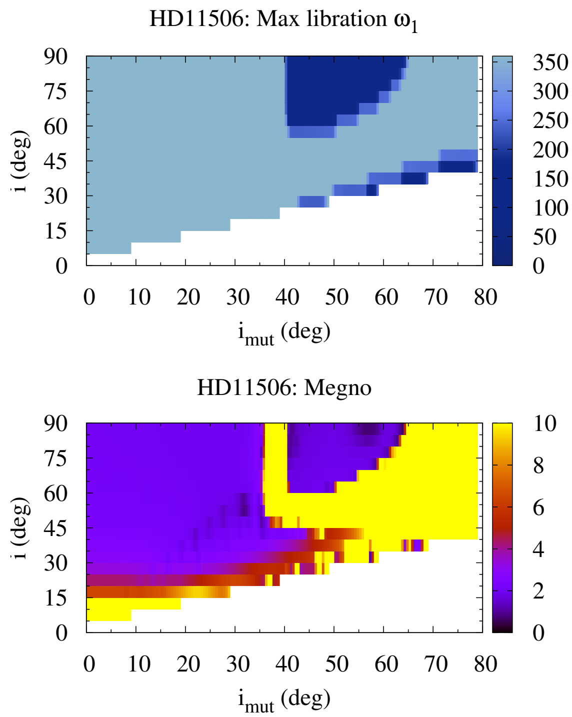

Figure 1: Parametric study of the system HD 11506. Top panel: maximal libration of ω_1. Bottom panel: MEGNO values.

Acknowledgements

M.V. acknowledges financial support from the FRIA fellowship (F.R.S.-FNRS). The work of A.R. is supported by a F.R.S.-FNRS research fellowship. Computational resources have been provided by the Consortium des Équipements de Calcul Intensif (CÉCI), funded by the Fonds de la Recherche Scientifique de Belgique (F.R.S.-FNRS) under Grant No. 2.5020.11.

References

[1] Cincotta, P. M. and Simo, C., Simple tools to study global dynamics in non-axisymmetric galactic potentials - I, Astronomy & Astrophysics, Vol. 147, pp. 205–228, 2000

[2] Kozai, Y., Secular perturbations of asteroids with high inclination and eccentricity, Astrophysical Journal, Vol. 67, pp. 591, 1962

[3] Libert, A.-S. and Sansottera, M., On the extension of the Laplace-Lagrange secular theory to order two in the masses for extrasolar systems, Celestial Mechanics & Dynamical Astronomy, Vol. 117, pp. 149–168, 2013

[4] Libert, A.-S. and Tsiganis, K., Kozai resonance in extrasolar systems, Astronomy & Astrophysics, Vol. 493, pp. 677-686, 2009

[5] Locatelli, U. and Giorgilli, A., Invariant tori in the secular motions of the three-body planetary systems, Celestial Mechanics & Dynamical Astronomy, Vol. 78, 2000

[6] Lidov, M. L., The evolution of orbits of artificial satellites of planets under the action of gravitational perturbations of external bodies, Planetary and Space Science, Vol. 9, pp. 719-759, 1962

[7] Robutel, P., Stability of the planetary three-body problem, Celestial Mechanics & Dynamical Astronomy, Vol. 62, pp. 219–261, 1995

EPSC Abstracts
Vol. 12, EPSC2018-282, 2018
European Planetary Science Congress 2018

On the geometry of forming encounter in two young asteroid pairs

A. Rosaev (1), N.I. Perov (1,2) and E. Plavalova (3)
(1) Cultural and Educational Centre named after V.V. Tereshkova, Yaroslavl, Russian Federation (hegem@mail.ru)
(2) State Pedagogical University named after K.D. Ushinskii, Yaroslavl, Russian Federation (perov@yarplaneta.ru)
(3) Mathematical Institute Slovak Academy of Sciences (plavalova @komplet.sk)

1. Introduction

The collisions of celestial bodies are of the great interest in modern planetary astronomy. It may be expected, that close encounters and collisions play an important role in dynamics of exoplanetary systems as well as in our Solar system. Here we consider a model of motion and approaching of the Solar system two asteroids.

2. Method

Based on the numerical integration of the nominal orbit with "Mercury" integrator [1], the following results were obtained for some young asteroid pairs (table 1). The age of the pairs obtained by us is close to that determined in the works [2, 3].
Asteroid radii can be estimated by Bowell's formula [4] through stellar magnitudes under the assumption of equal albedo A=0.288:

$$R(km) = \frac{1329}{2}\frac{10^{-H/5}}{\sqrt{A}}$$

Accepting the density value 2.7 g / cm^3, it is possible to estimate the mass of the main asteroid in the pair and then the radius of its sphere Hill (table 2). In both cases, we have a significant difference in mass, and we can apply a restricted 3-body model.

Table 1:

Asteroid		Dmin, au	Epoch, yr
6070 Rheinland	54827 (2001 NQ8)	0.000066	-16376.2
87887 (2000 SS286)	415992 (2002 AT49)	0.000026	-7209.9

Table 2:

Asteroid		H_1	H_2	R_1, km	R_{hill}, km
6070 Rheinland	54827 (2001 NQ8)	13.8	15.4	2.15	860
87887 (2000 SS286)	415992 (2002 AT49)	15.2	16.5	1.1	450

Hill sphere method is well known for studying stability of asteroid small satellite. If the mass of the smaller body (e.g. largest asteroid) is equal *m*, and it orbit around the Sun (of mass *M*) with a semi-major axis *a* and an eccentricity of *e*, then the radius *r* of the Hill sphere for the smaller body (e.g. asteroid primary) equals approximately **[5]:**

$$r_H \approx a(1-e)\sqrt[3]{\frac{m}{3M}}$$

3. Results

For the considered pairs, relative orbits of encounters were constructed. As a result, we obtained that the smaller asteroid quite a long time (about several years) is at a distance $5 \div 10\, r_H$ from the main asteroid of the pair. This demonstrates the importance to take into account mutual attraction in this case. It is shown at low relative velocities (cm/s), the mutual attraction may be significant outside the Hill sphere.
In addition, we performed numerical integration with a small variation in the initial orbital data of the asteroid 6070 Rheinland. As a result, we received a significant change in the geometry of the approaching at variations the semimajor axis ±3*10^{-9} AU (figure 1-2). Variations of the other elements did not play a significant role for the geometry of the encounter.

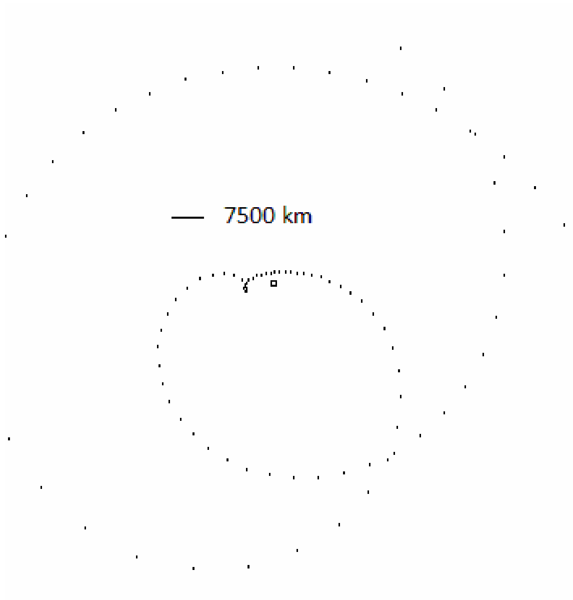

Figure 1: XY-projection of 6070 Rheinland and 54827 (2001 NQ8) encounters 16376 years ago (da=+3*10^{-9} AU)

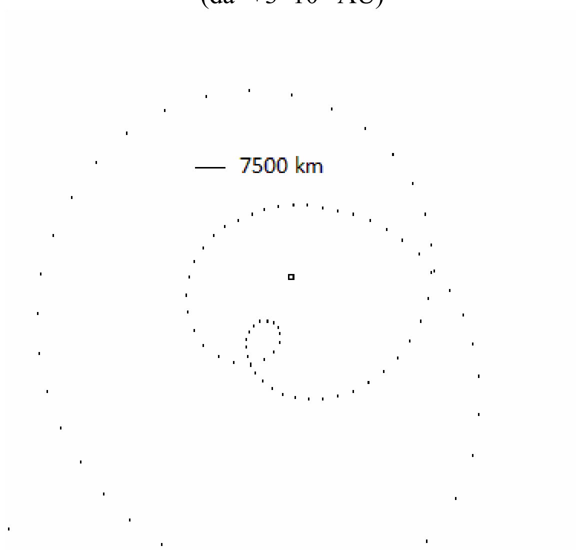

Figure 2: XY-projection of 6070 Rheinland and 54827 (2001 NQ8) encounters 16376 years ago (da=-3*10^{-9} AU)

4. Summary and Conclusions

Thus, we can draw the following conclusions: 1) it is necessary to take into account the mutual attraction of asteroids in close encounters in which they formed; 2) small variation of the initial semimajor axis can significantly change the geometry of the encounters.

References

[1] Chambers, J.E., 1999. A hybrid symplectic integrator that permits close encounters between massive bodies. Mon Not R Astron Soc 304, 793–799.

[2] Zizka J., Galad A., Vokrouhlicky D., Pravec P., Kusnirak P., Hornoch K.: Asteroids 87887 - 415992: the youngest known asteroid pair?, A&A 595, A20 (2016).

[3] Vokrouhlicky D., et al.: Detailed Analysis of the Asteroid Pair (6070) Rheinland and (54827) 2001 NQ8.,The Astronomical Journal, 153, 270-266, 2017.

[4] Bowell, E., Hapke, B., Domingue, D., Lumme, K., Peltoniemi, J., Harris, A.W., 1989. Application of photometric models to asteroids. In: Binzel, R.P., Gehrels, T., Matthews, M.S., (Eds.), Asteroids II, pp. 524–556.

[5] Hamilton D.P., Burns J.A. Orbital stability zones about asteroids. II - The destabilizing effects of eccentric orbits and of solar radiation., *Icarus* **96** (1), p. 43-64, (1992).

EPSC Abstracts
Vol. 12, EPSC2018-328, 2018
European Planetary Science Congress 2018

Approaching Preplanetary Streaming Instabilities in Laboratory Experiments

Niclas Schneider, Gerhard Wurm
University of Duisburg-Essen, Germany (niclas.schneider@uni-due.de)

Abstract

Streaming instabilities are an important particle concentration mechanism in protoplanetary disks but the idea is solely based on numerical simulations so far. We carried out first experiments to approach this mechanism in laboratory studies. We observed a particle cloud trapped in a rotating system under Earth's gravity. The experiment Stokes number is 0.0024. For average dust-to-gas ratios up to 0.02 particles behave like individual test particles. The sedimentation speed is identical to the calculated one. For larger dust-to-gas ratios the motion of particles gets sensitive to particle density and interparticle distances. This suggests a self-amplification of a denser region and provides a first step in supporting the concept of streaming instabilities.

1. Introduction

A major issue in planet formation theory is the radial-drift barrier. Solid particles in a protoplanetary disk would orbit around a star with Keplerian velocity, but the pressure-supported gas is about 50 m/s slower. This results in an aerodynamic drag and the headwind causes the solids to spiral inwards.
Streaming instabilities introduced by Youdin and Goodman (2005) are a promising way to overcome this barrier. In this mechanism, the drag produces a back reaction on the gas, leading to an increase in the gas velocity and a reduction of the aerodynamic drag. It has been shown in simulations, that this aerodynamic coupling between the gas and the particles can lead to clustering and a collective drag reduction and finally to the formation of planetesimals (Johansen and Youdin 2007; Yang et al. 2017).
In analogy to the relative velocity of dust and gas in a protoplanetary disk, we investigate spherical sedimenting particles trapped in a rotating cylindrical vacuum chamber at low pressure.

2. Experiment

2.1 Setup

The experiment chamber is 20 cm in diameter and is evacuated to a preset pressure at the beginning of the experiment. Inside the chamber a ring of LEDs generates light that is scattered from the particles which are imaged by a camera in the front. The particles are generated through a vibrating sieve, included in an extension of the vacuum chamber. This beam of particles has a width of 25 mm and a thickness of 5 mm. Particles are injected while the experiment is still at rest to fill the regions that allow stable (circular) particle trajectories once the rotation is started. A sketch of the experiment can be seen in fig. 1.

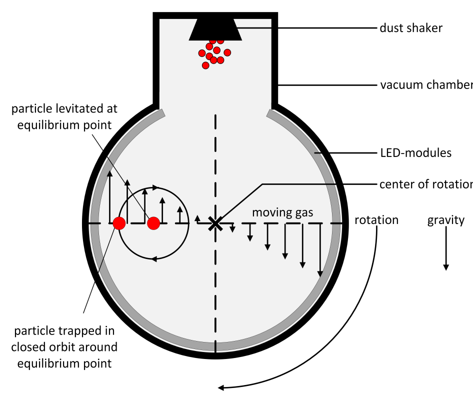

Figure 1: Schematics of the experiment. Not shown are auxiliary parts. The experiment chamber is a vacuum chamber evacuated prior to experiments to a preset pressure. A camera is observing particles from the front by scattered light.

2.2 Experimental parameters

For this first study we used hollow glass spheres to allow large non-sticky particles with low density for short gas-grain coupling times. The grains have an average diameter of 165 µm and a friction time of 7 ms. As gas we used air with a gas pressure of 2100 Pa.
We analyse the sedimentation velocity of the particles with respect to the average dust-to-gas ratio. Moreover, we defined the closeness C_i of particle i as

$$C_i = \sum_{n=1}^{N} \frac{1}{r_n - r_i} \tag{1}$$

to get an insight on local particle number densities. Be aware that the closeness is constructed from the distances between the individual particles $(r_n - r_i)$ and the total number of particles N. The dependence of the sedimentation velocity on the closeness is an indicator for a collective behaviour of the particles.

3. Grain Motion

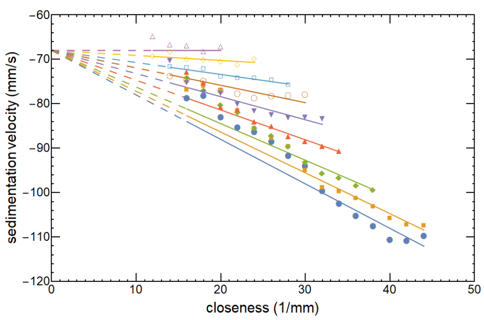

Figure 2: Sedimentation velocity over closeness for individual rotations of the experiment. The evolution within the experiment chamber goes from initially dense (lower data, 2nd round) to less dense (upper data, 10th round) cloud as particles diffuse to the chamber wall. Data are average values for typically several hundred particles

Particles in regions with high closeness sediment much faster than particles in less close regions as seen in fig. 2. This figure shows the values averaged over full rotations of the experiment, therefore increasing in time from 3 s (lower curve) to round 10 or 30 s (upper curve).
Visible in round 10 (fig. 2), particles at later times, on average in a less dense cloud, all sediment with the same speed even at a closeness 20 mm^{-1}. In contrast, in the high loading case, the speed of particles with the same closeness 20 mm^{-1} is increased. The speed is no longer constant but now depends on the closeness. Obviously the system is sensitive to closeness variations in this case. To a good approximation the dependence of the sedimentation speed on closeness can be described as linear or

$$v = v_0 - F_s \cdot C_i \tag{2}$$

The sensitivity factor F_s increases with the average solid-to-gas-ratio of the system above a threshold solid-to-gas ratio of 0.02. Below this value particles behave like individual grains independent of the closeness.
For dust-to-gas ratios above 0.02 particle motion does depend on closeness and shows much higher sedimentation speeds than individual grains.

For the high mass loading individual particles can change their motion by entering regions of high closeness, speeding up. However, they can also drop out again into a region of lower closeness. We do not see any concentration effect leading to a continuous local increase of particle density for longer than a few seconds.

4. Summary and Conclusions

For solid-to-gas ratios above 0.02 we see a collective behaviour of the particles. The sedimentation velocity of the dust grains depends on both, the closeness and the average solid-to-gas ratio. Overall, our experiments support - for the first time in laboratory research - the ideas underlying streaming instabilities.

Acknowledgements

This work is funded by DFG WU 321/16-1.

References

[1] Youdin, A. N. and Goodman, J.: Streaming instabilities in protoplanetary disks, The Astrophysical Journal, 2005

[2] Johansen, A. and Youdin, A.: Protoplanetary disk turbulence driven by the streaming instability: nonlinear saturation and particle concentration. The Astrophysical Journal, 2007

[3] Yang, C.-C., Johansen, A. and Carrera, D.: Concentrating small particles in protoplanetary disks through the streaming instability, Astronomy and Astrophyics, 2017

EPSC Abstracts
Vol. 12, EPSC2018-345, 2018
European Planetary Science Congress 2018

Destruction by Protoplanetary Winds - How Stable are Planetesimals?

Tunahan Demirci, Maximilian Kruss, Jens Teiser, Tabea Bogdan, Felix Jungmann, Niclas Schneider, and Gerhard Wurm
University of Duisburg-Essen, Faculty of Physics, Lotharstr. 1, 47057 Duisburg, Germany (tunahan.demirci@uni-due.de)

Abstract

In this work we study the wind induced erosion of spherical sub-mm sized glass beads at low gravity and low atmospheric pressure. Our experimental setup combines a centrifuge with a low pressure wind tunnel on a parabolic flight. We determined the threshold friction velocity in dependence of ambient pressure and gravity. This strongly constrains the region in protoplanetary disks where planetesimals built from pebbles are stable against erosion.

1. Introduction

The formation of planets is a process that involves a number of size scales. In the km-range planetesimals have to be formed. Current models predict that a planetesimal consists of a loose collection of mm to cm-sized dust aggregates. On such planetesimals self-gravity as well as cohesion are weak. In protoplanetary disks these small bodies move on Kepler orbits around the central star. They experience head winds of 50 m/s in the surrounding gas [1]. Depending on the ambient pressure this wind can be sufficient to lift dust aggregates and thus erode the planetesimal.

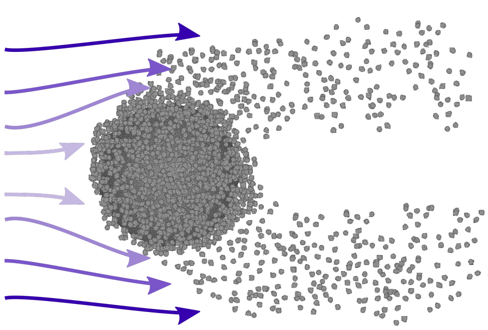

Figure 1: Planetesimals are destroyed under certain conditions of gas flow in protoplanetary disks.

2. Microgravity Experiments

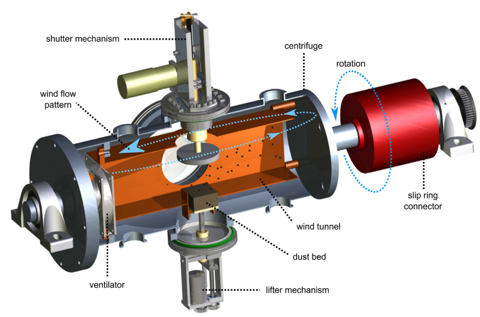

Figure 2: A schematic of the experimental setup [2]. The experiment combines a low pressure wind tunnel and a centrifuge.

We developed a parabolic flight experiment that combines a low pressure wind tunnel and a centrifuge. The wind tunnel is placed inside a vacuum chamber so we can operate it at various ambient pressures p from 10^{-1} to 10^{3} mbar. A fan inside the wind tunnel can generate a gas flow with velocities of up to 15 m/s. With this experiment we study the wind induced lift of dust and fine sand at different gravitational accelerations. The dust bed is placed at the bottom of the tunnel and is observed with a high-speed camera. The chamber which contains the wind tunnel also acts as a centrifuge. During microgravity of a parabolic flight we generate accelerations on the dust bed from 0.05 to 1 g with the centrifuge simulating different gravitational accelerations. On the recent parabolic flight campaign we have determined the threshold wind velocity u^* for spherical glass beads of diameter $d = 425 - 450\,\mu\mathrm{m}$ for gravitational accelerations between 0.11 and 0.22 g and ambient pressures between 3 and 12 mbar. The gas flow is just set high enough for lifting events to occur and the threshold friction velocity u^* is determined. Due to the linear height dependence of the flow velocity $u(h)$ within the viscous sublayer the threshold friction velocity can be calculated as

$$u^* = \sqrt{\frac{\eta}{\rho}\frac{\partial u(h)}{\partial h}}, \tag{1}$$

with the dynamic viscosity η and the gas density ρ. The height dependent gas flow velocity can be determined by the analysis of trajectories of lifted beads [3].

3. Wind Erosion

Several models predict the threshold conditions for particle lift going back to Bagnolds pioneering work [4]. The idea behind this model is that lift occurs if the gas drag force on the particle is greater than the particle's gravitational force. Shao and Lu [5] extended this model by considering the cohesion between the particles

$$u^* = A_N\sqrt{\frac{\rho_\mathrm{P}}{\rho}gd + \frac{\gamma}{\rho d}}. \tag{2}$$

This equation can be put into the form

$$\rho u^{*2} = A_N^2\left(\rho_\mathrm{P} gd + \frac{\gamma}{d}\right), \tag{3}$$

where the left side describes the gas properties and is proportional to the lift force. The right side of the equation is composed of gravity and cohesion which holds the particles on the bottom. Figure 3 shows the results of the recent parabolic flight campaign. Equation 3 is fitted to the data. The cohesion term is negligible in comparison to gravity for the used glass spheres, so that equation 2 can be reduced to

$$u^* \approx A_N\sqrt{\frac{\rho_\mathrm{P}}{\rho}gd}. \tag{4}$$

4. Summary and Conclusions

We have determined the threshold friction velocity u^* for spherical glass beads at low pressure p and low gravitational acceleration g. We have found that cohesion is negligible for the diameter of spheres which are used in the experiments. Assuming that compact dust agglomerates behave similar to solid glass beads of comparable size, a loose collection of mm to cm-sized dust aggregates are mainly hold together by gravity. Scaled to the pressure conditions in protoplanetary disks and the gravitational accelerations on surfaces of planetesimals the threshold friction velocity can be estimated with current models (see equation 4). The stability of planetesimals and the regions of stability within protoplanetary disks will be presented and discussed at the conference.

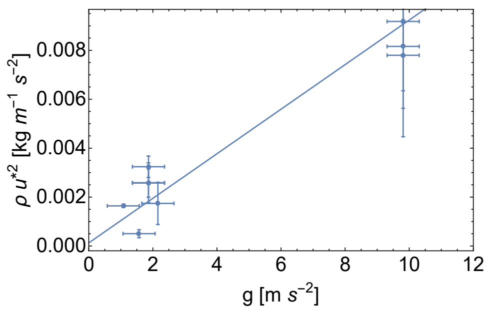

Figure 3: ρu^{*2} in dependence of the gravitational acceleration g.

Acknowledgements

This project is funded by DLR space administration with funds from the BMWi under grant 50 WM 1760. F. J. is funded by DLR space administration with funds from the BMWi under grant 50 WM 1542. M. K. is funded by the DFG, grant WU 321/14-1. N. S. is funded by the DFG grant WU 321/16-1.

References

[1] Johansen, A., Blum, J., Tanaka, H., Ormel, C., Bizzarro, M., Rickman, H.: The Multifaced Planetesimal Formation Process, Protostars and Planets VI (Tucson, AZ: Univ. Arizona Press), 547, 2014.

[2] Musiolik, G., Kruss, M., Demirci, T., Schrinski, B. Teiser, J., Daerden, F., Smith, M.D., Neary, L., Wurm, G.: Saltation under Martian gravity and its Influence on the global dust distribution, Icarus, 306, 25, 2018.

[3] Wurm, G., Blum, J., Colwell, J.E.: NOTE: a new mechanism relevant to the formation of planetesimals in the Solar Nebula. Icarus 151, 318–321, 2001.

[4] Bagnold, R. A.: The Physics of Blown Sand and Desert Dunes, Chapmann & Hll Ltd, London, 1941.

[5] Shao, Y. , Lu, H.: A simple expression for wind erosion threshold friction velocity. J. Geophys. Res. 105 (D17), 22437–22443, 2000.

EPSC Abstracts
Vol. 12, EPSC2018-376, 2018
European Planetary Science Congress 2018

Reproducing the Architecture of TRAPPIST-1 using Global Formation and Evolution Models

Remo Burn (1), Yann Alibert (1), Christoph Mordasini (1), Adrien Leleu (1) and Martin Schlecker (2)
(1) Physikalisches Institut, Universität Bern, Switzerland, (2) Max-Planck-Institut für Astronomie, Heidelberg, Germany
(remo.burn@space.unibe.ch)

Abstract

The, so far, unique and well constrained TRAPPIST-1 system can be exploited for testing planet formation theories. Because of observational biases, terrestrial planet formation models will, for the next decade, only be testable around low mass stars, showing the need for research in this area. We invoke the Bern model of global planet formation and evolution to conduct population syntheses for 0.1 $M_\odot$ stars and compare the wealth of systems to the TRAPPIST-1 system, finding reasonable consensus for many observables. However, compositions differ significantly.

1 Introduction

Since the discoveries of the first three [7] and later of at least four more [8] planets in the TRAPPIST-1 (T1) system, planet formation theories are challenged by the compactness of the system and the not well studied regime of low mass stars (0.08 $M_\odot$). A universal model of planet formation should be extendable to all regimes. Especially crucial is the extension to late-type stars because the detection probability of the prevalent techniques scales with the mass or radius ratio of the planet and its host star. Thus, the extreme case of T1 is an important benchmark case in terms of how processes are scaling with the stellar mass.

It is generally not expected for giant planets to form around very low mass stars. Therefore, the formation of the T1 system is mainly dependent on the assumed solid accretion and migration model and is not masked by the influence of giant gaseous planets, thus serving as a reference for those processes.

Especially challenging for formation models, even though not well constrained, are the compositions inferred from TTV-masses and the transit radii shown in Grimm et al. [9]. The variability in terms of composition could point to different formation locations, without, however, showing the typical gradient towards more volatile rich compositions with increasing orbital period. We resolve which system-wide compositional features can possibly be inherited from formation.

In contrast to the qualitative study by Ormel et al. [13] that proposes a possible pathway to form compact systems in the pebble accretion scenario, we focus on the planetesimal accretion model and perform quantitative calculations using the classical formation route.

Planet formation models in general are highly dependent on the disk initial conditions and the placement of seeds or embryos. In the population synthesis framework [4, 12], the initial conditions are randomized according to probability distributions suggested by observations of protoplanetary disks [10]. Drawing from this set of initial conditions, we first run our planet formation code for a generic 0.1 $M_\odot$ star. We then develop a criterion for similarity and apply it to search for systems resembling T1.

2 Methods

Our planet formation models are based on the models of Alibert et al. [1], adapted to the case of low mass stars. The models [1, 6, 12] include: an $\alpha = 10^{-3}$ viscous protoplanetary disk with irradiation of the star, type I and II orbital migration of the planets [5], accretion of planetesimals [6], solution of the spherically symmetric internal structure equations of the planets to obtain their gas accretion rate, planetary radius calculation based on the core composition [11], the N-body interaction between the forming (proto-) planets [1] and the evolution over time of the central star [3].

The models are computed for a 0.1 $M_\odot$ central star, which influences a number of processes and features, including the disk structure, the planetary radius during the nebular phase due to the changed Hill radius, migration timescales and the disk mass. Since we consider planets located very close to their parent star, the disk extends down to 0.01 AU in our models.

The initial disk profiles of the 1000 planetary system simulations follow the ones already used in [1], i.e. a power law disk with exponent $\gamma = 0.9$ with an exponential cutoff radius a_{C}. The total disk mass distribution is derived from observations [2], but it is scaled down compared to the one for solar-type stars following a linear scaling law $M_{\mathrm{disk}} \propto M_{\mathrm{star}}$, which in turn scales $a_{\mathrm{C}} \propto M_{\mathrm{disk}}^{5/8}$ [2].

To account for small body drift, we use a steeper slope $\gamma_{\mathrm{p}} = 1.5$ and a lower cutoff radius $a_{\mathrm{C,p}} = 0.5 a_{\mathrm{C}}$ for the planetesimal disk than for the gas disk.

The disk lifetime is assumed not to depend on the mass of the central star, we use a mean lifetime of 3 Myr.

We assume that 50 proto-planets grow in the same protoplanetary disk, starting after 200 kyr in which planetesimals had time to form. The initial mass of the planetary embryos is 0.01 $M_{\oplus}$, and the initial location of each is drawn from a log-uniform distribution within 0.02 AU and 10 AU.

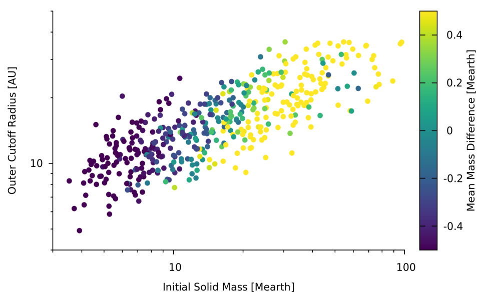

Figure 1: Initial conditions of systems with the mean mass of the synthetic system minus the mean mass of TRAPPIST-1 as color code. Considered were only synthetic planets with masses above 0.1 $M_{\oplus}$ and semi-major axes lower than 0.1 AU.

3 Results and Conclusions

We compare our synthetic planetary systems to T1 using different measures and find that many features of the T1 systems can be reproduced. We found similar mean motion resonances, mean masses and semi-major axes. For the mean mass, we find a region in initial solid mass and disk dimension that is favorable for the formation of a system similar to T1 (figure 1). This region of the parameter space partially overlaps with favorable regions in terms of other measures. However, the ice mass fraction in the synthetic planets is generally higher than the one inferred from TTV masses for the actual T1 planets [9] due to migration from regions outside the snowline. Matching the ice fractions seems to need fine-tuning of the model or consideration of additional processes, such as a low ice fraction outside the snow line or desiccation of planetesimals by a different heat source.

Acknowledgements

This work has been carried out within the frame of the National Centre for Competence in Research PlanetS supported by the Swiss National Science Foundation. The authors acknowledge the financial support of the SNSF.

References

[1] Alibert, Y., Carron, F., Fortier, A., et al, A&A, 558, A109, 2013.

[2] Andrews, S., Wilner, D., Hughes, A., et al, The Astrophysical Journal, 723, pp. 1241–1254, 2010.

[3] Baraffe, I., Homeier, D., Allard, F. and Chabrier G., A&A, 577, A42, 2015.

[4] Benz, W., Ida, S., Alibert, Y., et al, Protostars and Planets VI, University of Arizona Press, 2014.

[5] Dittkrist, K.-M., Mordasini, C., Klahr, H., et al, A&A, 567, A121, 2014.

[6] Fortier, A., Alibert, Y., Carron, F., et al, A&A, 549, A44, 2013.

[7] Gillon, M., Jehin, E., Lederer, S., et al., Nature, 533, p. 221, 2016.

[8] Gillon, M., Triaud, A. H. M. J., Demory, B.-O., et al., Nature, 542,p. 456, 2017.

[9] Grimm, S. L., Demory, B.-O., Gillon, M., et al, A&A, in press, 2018.

[10] Mordasini, C., Alibert, Y., Benz, W., A&A, 501, pp. 1139-1160, 2009.

[11] Mordasini, C., Alibert, Y., Georgy, C., et al, A&A, 547, A112, 2012.

[12] Mordasini, C., arXiv:1804.01532, Invited review accepted for publication in the 'Handbook of Exoplanets', 2018.

[13] Ormel, C. W., Liu, B., & Schoonenberg, D., A&A, 604, A1, 2017.

EPSC Abstracts
Vol. 12, EPSC2018-400, 2018
European Planetary Science Congress 2018

Layered semi-convection and Tides in giant planet interiors

Quentin André (1), Stéphane Mathis (1, 2) and Adrian J. Barker (3)
(1) Laboratoire AIM Paris-Saclay, CEA/DSM – CNRS – Université Parid-Diderot, IRFU/SAp Centre de Saclay, 91191 Gif-sur-Yvette, France (quentin.andre@cea.fr)
(2) LESIA, Observatoire de Paris, CNRS UMR 8109, UPMC, Université Paris-Diderot, 5 place Jules Janssen, 92195 Meudon, France
(3) Department of Applied Mathematics, School of Mathematics, University of Leeds, Leeds, LS2 9JT, UK

Abstract

Layered semi-convection could operate in giant planets, potentially explaining Saturn's luminosity excess and playing a role in causing the abnormally large radii of some hot Jupiters. In giant planet interiors, it could take the form of density staircases, which are convective layers separated by thin stably stratified interfaces. In addition, the efficiency of tidal dissipation is known to depend strongly on the planetary internal structure. It is crucial to improve our understanding of the mechanisms driving this dissipation, since it has important consequences to predict the long-term evolution of any planetary system. In this work, our goal is to study the resulting tidal dissipation when internal waves are excited by other bodies (such as the moons of giant planets) in a region of layered semi-convection. We find that the rates of tidal dissipation can be enhanced in a region of layered semi-convection compared to a uniformly convective medium, where the latter corresponds with the usual assumption adopted in giant planet interior models. In particular, a region of layered semi-convection possesses a richer set of resonances, allowing enhanced dissipation for a wider range of tidal frequencies. Thus, layered semi-convection could contribute towards explaining the high tidal dissipation rates observed in Jupiter and Saturn, which have not yet been explained by theory. Further work is required to explore the efficiency of this mechanism in global models.

1 A first study of tidal dissipation in layered semi-convection

1.1 Context

It has been found that the rates of tidal dissipation in Jupiter and Saturn are higher than previously thought

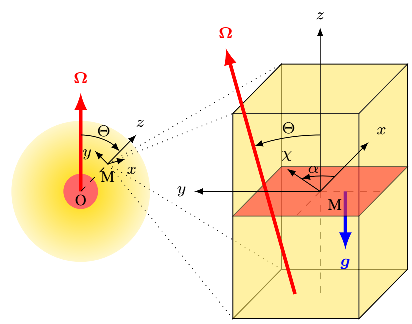

Figure 1: Our local Cartesian model.

(1; 2; 3). This has important astrophysical consequences since tidal interactions are a key mechanism for driving the rotational, orbital and thermal evolution of moons, planets and stars over very long timescales. Moreover, we know that this evolution, linked to the efficiency of tidal dissipation in celestial bodies, strongly depends on their internal structures. Recent observations by the JUNO spacecraft seem to be consistent with interior models of Jupiter in which the heavy elements of the core are diluted in the envelope (4). This could lead to the development of layered semi-convection , in which a large number of convective layers are separated by thin stably stratified interfaces. In this work, we study the impact of layered semi-convection upon the efficiency of the so-called dynamical tide, that is the viscous and thermal dissipation of tidal waves.

1.2 Dissipation rates in a layered profile

To simplify our initial study, and because tidal waves typically have very short wavelengths, we carry out our analysis in a local Cartesian box centred on a given point M of the fluid envelope (see Fig. 1). This al-

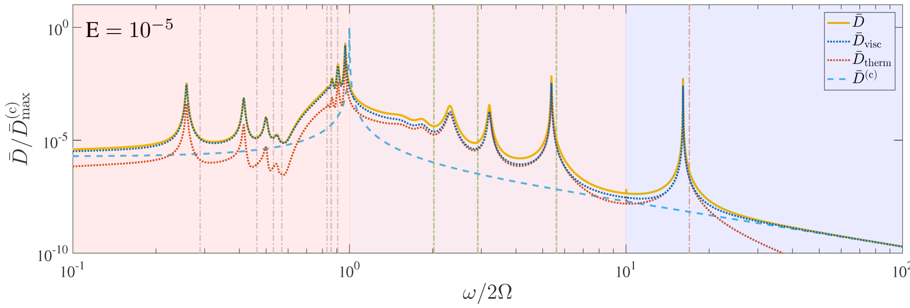

Figure 2: Example of a normalised dissipation as a function of tidal frequency for an Ekman number $\mathrm{E} = 10^{-5}$.

lows us to study the local properties of the propagation and dissipation of internal waves in a region of layered semi-convection. We take into account rotation through the Coriolis acceleration (the rotation vector is $\mathbf{\Omega}$ on Fig. 1), and the region of layered semi-convection is modelled by a buoyancy frequency profile, $N(z)$, that is zero in the convective regions and positive in stably stratified interfaces. The mean stratification in the vertical direction is then $\bar{N}$. Finally, viscous and thermal are included through constant kinematic viscosity ν and thermal diffusivity κ.

We give an example of our results focusing on the case with one stably stratified interface in the middle of our box, with the dissipation being characterised by choosing $\nu/2\Omega = \kappa/2\Omega = 10^{-5}$. The dissipation rates calculated numerically are plotted as a function of tidal forcing frequency on Fig. 2. The total dissipation rate, $\bar{D}$, is represented by the solid orange line (its viscous and thermal contributions are represented by the dotted blue and red lines, respectively). For comparison, we plot the corresponding quantity in a fully convective medium, $\bar{D}^{(c)}$ by the dashed light blue line.

We clearly see here that the layered structure introduces new resonances. Those additional resonances are broadly distributed over the frequency spectrum. Some correspond to resonances with inertial modes, corresponding to frequencies $\omega \lesssim 2\Omega$ (pink region on Fig. 2); some with super-inertial gravito-inertial modes, corresponding to frequencies $2\Omega \lesssim \omega \lesssim \bar{N}$ (purple region on Fig. 2); and finally some with gravity modes, corresponding to frequencies $\bar{N} \lesssim \omega \lesssim \max N$ (blue region on Fig. 2). As a result, the total dissipation rate is higher in the layered case (orange line) than in the fully convective case (dashed light blue line) – in particular in the sub-inertial range ($\omega < 2\Omega$) relevant to tidal forcing – except near the Coriolis frequency ($\omega \sim 2\Omega$).

1.3 Conclusions

We computed the dissipation rates in a region of layered semi-convection as a function of tidal frequency using a local Cartesian model. We found that a region of layered semi-convection possesses a richer set of free modes than a fully convective medium – which is the model that is usually adopted for giant planet interiors. As a result, there are more resonances that can potentially be excited compared to a convective medium. This makes it more likely for a satellite to enter a resonance with enhanced tidal dissipation (potentially by several orders of magnitude). Further work is required to explore and confirm the influence of layered semi-convection on tidal dissipation in global models.

Acknowledgements

QA and SM acknowledge funding by the European Research Council through ERC SPIRE grant 647383. AJB was supported by the Leverhulme Trust through the award of an Early Career Fellowship and by STFC Grant ST/R00059X/1.

References

[1] Lainey, V., Arlot, J.-E., Karatekin, Ö., & van Hoolst, T. 2009, Nature, 459, 957

[2] Lainey, V., Jacobson, R. A., Tajeddine, R., et al. 2017, Icarus, 281, 286

[3] Lainey, V., Karatekin, Ö., Desmars,J., et al. 2012, ApJ, 752, 14

[4] Wahl, S. M., Hubbard, W. B., Militzer, B., et al. 2017, Geophys. Res. Lett., 44, 4649

EPSC Abstracts
Vol. 12, EPSC2018-426, 2018
European Planetary Science Congress 2018

Evolution of trojan exoplanets in protoplanetary discs

Adrien Leleu (1,2), Gavin Coleman (1) and Sareh Ataiee (3)
(1) Physics Institute, Space Research and Planetary Sciences, Center for Space and Habitability - NCCR PlanetS - University of Bern, Switzerland
(2) IMCCE, Observatoire de Paris - PSL Research University, UPMC Univ. Paris 06, Univ. Lille 1, CNRS, 77 Avenue Denfert-Rochereau, 75014 Paris, France
(3) Institut für Astronomie und Astrophysik, Computational Physics, Auf der Morgenstelle 10, 72076 Tübingen, Germany
(adrien.leleu@space.unibe.ch)

Abstract

Despite the existence of co-orbital bodies in the solar system, and the prediction of the formation of co-orbital planets by planetary system formation models, no co-orbital exoplanets (also called trojans) have been detected so far. We investigate how a pair of trojan exoplanets would fare during their migration in a protoplanetary disc. To this end, we start with an analytical study of the evolution of two planets near the Lagrangian equilibria L_4 and L_5, identifying for which values of the parameters these equilibria are either attractive or repulsive. We then compare these results to hydrodynamical simulations. Finally, we study the evolution of co-orbital configurations using a planetary system formation model that simulates the orbital evolution of the planet over the disc lifetime. Depending on the parameters of the disc, and the orbital parameters and masses of the planets, the system can either evolve toward the Lagrangian equilibrium, or tend to increase its amplitude of libration, possibly all the way to horseshoe orbits or even exiting the resonance. The stability in the direction of the eccentricities and the inclinations is also studied.

1. Introduction

Celestial bodies in co-orbital configurations are common in the solar system: the Earth, Mars, Jupiter, Uranus and Neptune have known co-orbital asteroids (also called trojans in the case of Jupiter). Two bodies of comparable masses can be in a co-orbital configuration as well: it is the case of the Saturnian moons Janus and Epimetheus, that have a mass ratio of ≈ 3.5 and are on a horseshoe orbit around Saturn. Co-orbital exoplanets are a common outcome of planetary system formation models [1,2], which typically yield co-orbital exoplanets in a few percent up to a few tens of percent of the created systems. All that being said, no co-orbital exoplanets have been found so far, despite survey missions such as Kepler that found hundreds of multi-planetary systems. Potential observational biases and adapted detection method were discussed in previous studies [3,4]. Here we discuss how dissipation affects the co-orbital resonance, particularly in the case of migration in protoplanetary discs, for small inclinations and eccentricities.

2. Method

Using the formalism developed in [5], we start by studying the behaviour of this resonance in the vicinity of the L_4 and L_5 Lagrangian equilibria. We develop an analytical model of the co-orbital resonance with a generic form of dissipation:

$$\begin{aligned} \dot{a}_j &= -a_j/\tau_{a_j} = -a_j/(\tau_{w_j} a_j^k)\,, \\ \dot{e}_j &= -e_j/\tau_{e_j}\,, \\ \dot{I}_j &= -I_j/\tau_{I_j}\,, \end{aligned} \tag{1}$$

where a, e, I are the semi-major axes, eccentricities, and inclinations of the planets, and the τ are migration and damping timescales. We then study the stability of the L_4 and L_5 equilibria in three directions: the 'circular' direction, associated to the semi-major axis and resonant angle; the direction associated with the eccentricities; and the one associated with the inclinations. Depending on the value of the masses of the co-orbitals and the strength of the dissipation of the different orbital elements, we show that the system can evolve toward the equilibria, or away from them, in the various directions.

In order to apply these results to the evolution of planets in protoplanetary discs, we study the evolution of co-orbital planets in the disc using short-duration 2-D hydrodynamic simulations. In this set of simulations, we explore the indirect effect of the planets on one another through perturbation of the protoplanetary discs. Two cases are studied: the type 1 migration, where both planets are embedded in the disc, and the type 2 migration, where one or both planets opened a gap in the disc.

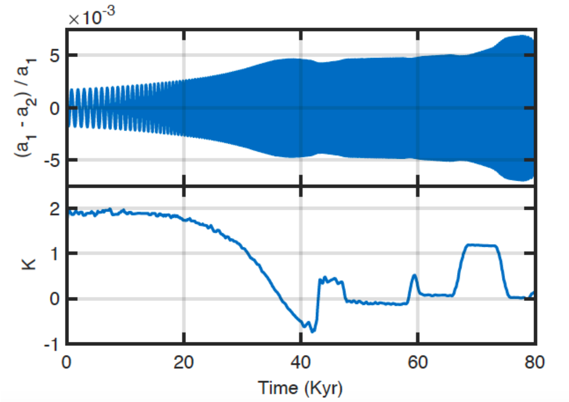

Figure 1: Top: libration around the exact resonance for a pair of coorbitals ($m_1 = 2m_2 = 20m_{Earth}$) embedded in a protoplanetary disc that evolves in time. Bottom: value of the parameter k, function of the disc parameters. For this value of the masses, the Lagrangian equilibria are attractive when $k < 0$, and repulsive otherwise.

Finally, we study the behaviour of co-orbital configurations in a 1-D evolving disc, that simulates the orbital evolution of the planet throughout the disc lifetime. We again study both types of planet migration, but over a much larger timescale than is computationally feasible for hydrodynamic simulations. The larger time-scales allow us to follow the evolution of the co-orbital planets as they migrate into different regions of the disc, which can have vastly different dissipation rates that thus significantly affect the evolution of the co-orbital system (Figure 1).

Acknowledgements

The authors acknowledge support from the Swiss NCCR PlanetS and the Swiss National Science Foundation.

3. Results

For given masses of the planets we identified for which value of the parameter k (defined in equation 1) the Lagrangian equilibria are attractive or repulsive.

In the case of type 1 migration, k is a function of the local disc density profile and temperature profile. In this regime, the behaviour of the co-orbital resonance is hence predictable from the parameters of the disc and the mass of the planets (Figure 1). In type 2 migration, our analysis rely mainly on the result of the hydrodynamical simulations.

This work hence allows to identify general trends, such as the range of expected amplitude of libration for the resonant angle as a function of the mass of the planets. In certain cases, evolution toward inclined co-orbitals, or eccentric ones, is also possible. These results help to explain the absence of certain configuration of co-orbital exoplanets, and might prove useful to develop adapted detection methods for the hunt for the first co-orbital exoplanet [6].

References

[1] Coleman, G. A. L. and Nelson, R. P.: Giant planet formation in radially structured protoplanetary discs, MNRAS, vol. 460 (2016)

[2] Cresswell, P. & Nelson, R. P.: Three-dimensional simulations of multiple protoplanets embedded in a protostellar disc A&A, 482, 677 (2008)

[3] Leleu, A., Robutel, P. and Correia, A. C. M.: Detectability of quasi-circular co-orbital planets. Application to the radial velocity technique. Astron. Astrophys., 581:A128 (2015).

[4] Leleu, A., Robutel, P. Correia, A. C. M., and Lillo-Box J.: Detection of co-orbital planets by combining transit and radial-velocity measurements, Astronomy & Astrophysics 599, L7 (2017)

[5] Robutel, P. and Pousse, A.: On the co-orbital motion of two planets in quasicircular orbits. Celest. Mech. Dyn. Astron., 117:17–40 (2013)

[6] Lillo-Box J. et al.: The Troy project: Searching for co-orbital bodies to known planets, Astronomy & Astrophysics vol. 609 (2018)

EPSC Abstracts
Vol. 12, EPSC2018-439, 2018
European Planetary Science Congress 2018

Tidal dissipation in the host star of short-period exoplanetary systems

Stéphane Mathis (1), Emeline Bolmont (1), Florian Gallet (2,3), Cilia Damiani (4), Corinne Charbonnel (3), Louis Amard (5,3), Yann Alibert (6)

(1) Laboratoire AIM Paris-Saclay, CEA/DRF - CNRS - Univ. Paris Diderot - IRFU/DAp, Centre de Saclay, 91191, Gif-sur-Yvette Cedex, France; (2) Université Grenoble Alpes, CNRS, IPAG, 38000 Grenoble, France; (3) Department of Astronomy, University of Geneva, Chemin des Maillettes 51, 1290, Versoix, Switzerland; (4) Max-Planck-Institut für Sonnensystemforschung, Göttingen, Germany; (5) University of Exeter, Department of Physics & Astronomy, Stoker Road, Devon, Exeter, EX4 4QL, UK 0000-0001-9590-2274; (6) Physikalisches Institut & Center for Space and Habitability, University of Bern, Sidlerstrasse 5, 3012, Bern, Switzerland (stephane.mathis@cea.fr)

Abstract

With the successes of the space missions CoRoT, *Kepler*, and K2 and of the large ground-based surveys, we are living a revolution for our knowledge of planetary systems. As of today, more than 2950 confirmed exoplanets have been discovered. They orbit a broad diversity of host stars with different masses and evolutionary stages.

In this context, many systems have a compact orbital architecture with planets orbiting very close to their star. Such systems, which will be explored by CHEOPS, TESS and SPIRou, are the seat of strong tidal (and magnetic) interactions. They modify the orbits of the planets and the stellar and planetary rotation angular velocity and inclination. In the case of stable binary systems, they lead to the orbit circularisation and to the spins synchronisation and alignment; in the case of unstable systems they drive the spiraling of the planet towards the central star. In short-period systems, this is the dissipation of tidal flows and waves excited in the host star that drive these processes.

In this work, we review the efforts that we have achieved to model stellar tides and their dissipation in the convective envelope of low-mass stars. We show how this tidal friction is intrinsically driven by the structural and rotational evolution of stars and how it strongly impacts the evolution of their planetary system. We also discuss the perspectives of this work to take into account the dissipation of tides in stellar radiation zones and the effects of differential rotation and magnetic fields.

1. General motivation

The broad diversity of the orbital architecture of discovered short-period exoplanetary systems stimulates a lot of studies of their dynamical evolution and stability. In this framework, tidal interactions are one of the key physical mechanisms that must be understood and coherently modeled. Indeed, the dissipation of the kinetic energy of tidal large-scale flows and waves in the host star of short-period exoplanetary systems drives the evolution of the semi-major axis and the eccentricity of the orbits, of their rotation, and of the spin-orbit inclination. In this framework, a large number of studies proposed to use the simplified so-called tidal quality factor Q to parametrize the efficiency of this dissipation and the related friction. Using the phenomenology of forced damped oscillators, the dissipation is strong and the evolution is rapid when the quality factor is small and vice-versa. Two ways are then used to prescribe a value for Q: i) one can choose to calibrate it on observations or on formation scenario ; ii) one choose to compute it using ab-initio hydrodynamical models of dissipative mechanisms acting on tidal flows (e.g. Ogilvie & Lin 2007, Ogilvie 2013). In the second case, tidal dissipation becomes a complex function of the internal structure of stars, of their dynamical properties (their rotation, stratification, viscosity and thermal diffusivities, etc.) and of the forcing frequency. Such dependences have a strong impact on the dynamical evolution of systems.

To obtain a coherent picture of the dynamics of exoplanetary systems it is thus necessary to have a correct evaluation of tidal dissipation in their host stars along their evolution. From now on, stellar mass range spreads from M red dwarfs to intermediatemass A-type stars. In this context, tidal friction in the rotating turbulent convective envelopes of these low-mass stars has been proposed to explain the orbital and rotational properties of hot-Jupiter systems (e.g. Albrecht et al. 2012, Valsecchi & Rasio 2014, and references therein for hot-Jupiter systems). In stellar convective layers, tidal flows are constituted of large-scale non-wavelike/equilibrium flows driven by the adjustment of the hydrostatic structure of stars because of the presence of the planetary companion and the dynamical tide constituted by inertial waves, which have the Coriolis acceleration as restoring force (e.g. Ogilvie & Lin 2007). In addition, both the structure and rotation of stars strongly vary along their evolution (e.g. Amard et al. 2016) while observations of star-planet and binary-star systems show that tidal dissipation varies over several orders of magnitude. Therefore, the key questions that must be addressed for dynamical studies is how does the tidal friction in the convective envelope of low-mass stars vary as a function of stellar mass, evolutionary stage, and rotation?

2 Results

Combining the formalism derived for the frequency-averaged dissipation of tidal inertial waves propagating in convective regions of stars (Ogilvie 2013) with state-of-the-art grids of stellar rotating models (Amard et al. 2016), we show that:

- the stellar tidal friction is a complex function of the mass, metallicity, age, and rotation (Mathis 2015, Gallet et al. 2017, Bolmont et al. 2017);
- it varies over several orders of magnitude as a function of these physical parameters;
- it is driven by the evolution of the stellar structure during the pre-main-sequence and by the evolution of rotation during the main-sequence;
- the predicted orbital migration and planet survival rate obtained using such an ab-initio modeling is strongly different that the one assuming a constant tidal quality factor (Bolmont & Mathis 2016);
- tidal dissipation cannot explain the dichotomy observed for the exoplanetary spin-orbit angles (Damiani & Mathis 2018).

Acknowledgements

S.M. and E.B. acknowledge funding by the European Research Council through ERC grant SPIRE 647383. E.B. acknowledges that this work is part of the F.R.S.-FNRS ExtraOrDynHa research project. F.G., C.C., and L.A. acknowledge financial support from the Swiss National Science Foundation (FNS) and from the SEFRI project C.140049 under COST Action TD 1308 Origins. This work was also supported by the ANR Blanc TOUPIES SIMI5-6 020 01, the Programme National de Planétologie (CNRS/INSU), the Programme National de Physique Stellaire PNPS (CNRS/INSU), and PLATO CNES grant at Départment d'Astrophysique (CEA-Saclay). C.D. acknowledges funding from the ANR (Agence Nationale de la Recherche, France) program IDEE (ANR-12-BS05-0008) "Interaction Des Etoiles et des Exoplanètes", and from the German Space Agency (Deutsches Zentrum für Luftind Raumfahrt) under PLATO grant 50OO1501.

References

[1] Ogilvie, G., Lin, D. N. C., The Astrophysical Journal, Vol. 661, p. 1180-1191, 2007.

[2] Ogilvie, G., Monthly Noticies of the Royal Astronomical Society, Vol. 429, p. 613-632, 2013.

[3] Albrecht, S., et al., The Astrophysical Journal, Vol. 757, 18, 2012.

[4] Valsecchi, F., Rasio, F. A., The Astrophysical Journal, Vol. 786, 102, 2014.

[5] Amard, L., Palacios, A., Charbonnel, C., Gallet, F., Bouvier, J., Astronomy & Astrophysics, Vol. 587, 105, 2016.

[6] Mathis, S., Astronomy & Astrophysics, Vol. 580, L3, 2015.

[7] Gallet, F., Bolmont, E., Mathis, S., Charbonnel, C., Amard, L., Astronomy & Astrophysics, Vol. 604, 112, 2017.

[8] Bolmont, E., Gallet, F., Mathis, S., Charbonnel, C., Amard, L., Alibert, Y., Astronomy & Astrophysics, Vol. 604, 113, 2017.

[9] Bolmont, E., Mathis, S., Celestial Mechanics and Dynamical Astronomy, Vol. 126, pp. 275-296, 2016.

[10] Damiani, C., Mathis, S., Astronomy & Astrophysics, in press, eprint arXiv:1803.09661, 2018.

EPSC Abstracts
Vol. 12, EPSC2018-516, 2018
European Planetary Science Congress 2018

Migration of bodies to the Earth from different distances from the Sun

Sergei I. Ipatov
Vernadsky Institute of Geochemistry and Analytical Chemistry of Russian Academy of Sciences, Moscow, Russia
(siipatov@hotmail.com, http://siipatov.webnode.ru/)

Abstract

Probabilities of collisions with the Earth for bodies with initial eccentricities equaled to 0.3 were calculated for different initial semi-major axes from 2 to 40 AU. The probabilities calculated for 250 bodies can differ by up to a factor of several tens for different runs with similar orbits. For 1500 bodies in each series of calculations, the probability of a collision of one body with the Earth was about 4.1×10^{-6} for the disk between 5 and 7.5 AU, and it was 2.5×10^{-6} for the disk between 7.5 and 10 AU. On average, for the region between 20 and 35 AU the probability could exceed 10^{-6}. For bodies initially located in the asteroid belt, the probabilities of their collisions with the Earth were about 10^{-4}-10^{-3}, i.e., were much greater than for bodies initially located beyond Jupiter's orbit.

1. Introduction

In order to study the delivery of water and volatiles to the Earth one need to know the probabilities of collisions with the Earth for bodies migrated to the Earth from different distances from the Sun, located beyond the snow line. In our previous papers, we studied the probability p_E of a collision of a body with the Earth for bodies with orbits close to known Jupiter-family comets [3-7] and for planetesimals from the feeding zone of Jupiter and Saturn (with initial semi-major axes a from 4.5 to 12 AU, a number of initial planetesimals proportional to $a^{1/2}$, and initial eccentricities and inclinations equaled to 0.3 and 0.15 rad, respectively) [9]. The mean values of p_E were obtained to be about 2×10^{-6} for the planetesimals, and they usually exceeded 4×10^{-6} for the considered Jupiter-family comets. If migrating objects consisted half of water, then the total amount of water delivered to the Earth is about the mass of Earth's oceans at p_E=2×10^{-6} and at the total mass of planetesimals equaled to 200 Earth masses. The ratio of probabilities of collisions of bodies with a planet to the mass of the planet for Venus was about the same as that for the Earth, and that for Mars was greater by a factor of 2 or 3 than that for the Earth. Below I study the probabilities of collisions of bodies migrated to the Earth from different distances from the Sun.

2. Initial data used for calculations

Several series of calculations of migration of bodies under the gravitational influence of planets (from Venus to Neptune) have been made. The symplectic code from the Swift integration package [8] was used. In some runs, initial semi-major axes were the same and equaled r_f. In other runs, initial semi-major axes varied from a_{min} to a_{max}, where a_{max}-a_{min}=2.5 AU. For different runs, a_{min} varied from 2 to 40 AU with a step equaled to 2.5 AU. Initial eccentricities and inclinations equaled to 0.3 and 0.15 rad, respectively. Such eccentricities could be reached due to mutual gravitational influence of planetesimals during evolution of a disk of planetesimals in the feeding zone of the giant planets [1-2]. Integrations were made until bodies reached 2000 AU or collided with the Sun. However, some runs were stopped after a few tens of millions of years (typically after more than at 10^8 years), if p_E finished increasing during some time. In principle, p_E could increase after that stopping time, and so the lower limits of p_E are presented below. For each run, 250 bodies with different orientations of initial orbits were considered. For several runs, initial data could be the same, but the difference was only in a step of integration.

3. Results of calculations

Studies of migration of bodies with initial orbits close to those of Jupiter-family comets showed [3-6] that the value of p_E for one body could be greater than the sum of p_E for thousands of bodies with almost the same initial orbits. A few migrating bodies could move in Earth-crossing orbits during many millions of years, and they could provide the major contribution to the mean value of p_E calculated for thousands of bodies with close initial orbits. Some bodies did not reach the Earth's orbit during their dynamical lifetimes.

Similar results on the role of a few bodies in p_E have been obtained in new series of runs. The values of p_E could differ by a factor of several tens for the runs with the same initial orbits, but with a different step of integration. At the series of runs with a_{min}=5 AU, p_E varied from 2.4×10^{-7} to 8.5×10^{-6} for different runs, and $p_E=4.1\times10^{-6}$ for a series of 6 runs with 1500 bodies. At the series with a_{min}=7.5 AU, in one run p_E=0, in another run $p_E=1.15\times10^{-5}$, and $p_E=2.5\times10^{-6}$ for a series of 6 runs with 1500 bodies. At a_{min}=12.5 AU, p_E was about 2×10^{-6} for a series of 2 runs with 500 bodies.

On average, values of p_E were greater for smaller a_{min}, but due to a wide range of possible values of p_E for runs with the same initial data, one need to consider a greater number of runs for each a_{min} before making accurate estimates. For most runs with $a_{min}\geq20$ AU, it was obtained that $p_E<10^{-6}$. However, there were runs with greater values of p_E. For example, $p_E=7.2\times10^{-6}$ at a_{min}=22.5 AU and $p_E=1.5\times10^{-6}$ at a_{min}=32.5 AU. On average, for the region 20 - 35 AU the value of p_E could exceed 10^{-6}. The region could play a valuable role in migration of icy bodies to the Earth. In some above runs, p_E continued to grow after 50 Myrs.

For runs with a_{min}=2 AU and r_f=2.5 AU, the values of p_E were about 10^{-3}, i.e. were much greater than for bodies located at more than 5 AU from the Sun. In runs with a_{min}=2.5 AU, p_E was up to 7×10^{-5}. The values of p_E for such runs could grow after 100 Myrs.

Probabilities of collisions with the Moon for bodies migrated from beyond Jupiter's orbit usually were by about a factor of 16 or 17 smaller than probabilities of collisions with the Earth.

Acknowledgements

The work was supported by the Program of Fundamental Studies of the Presidium of RAS № 17 as a part of Russian state program for GEOKHI N 00137-2018-0030.

References

[1] Ipatov, S.I.: Accumulation and migration of the bodies from the zones of giant planets, Earth, Moon, and Planets, Vol. 39, pp. 101-128, 1987.

[2] Ipatov, S.I.: Migration of celestial bodies in the solar system, Editorial URSS Publishing Company, Moscow, 320 p., 2000, in Russian. http://www.rfbr.ru/rffi/ru/books/o_29239.

[3] Ipatov, S.I. and Mather, J.C.: Migration of Jupiter-family comets and resonant asteroids to near-Earth space, "Astrodynamics, Space Missions, and Chaos", ed. by E. Belbruno, D. Folta, and P. Gurfil, Annals of the New York Academy of Sciences, Vol. 1017, pp. 46-65, 2004. http://arXiv.org/format/astro-ph/0308448.

[4] Ipatov S.I. and Mather J.C.: Comet and asteroid hazard to the terrestrial planets, Advances in Space Research, Vol. 33, pp. 1524-1533, 2004. http://arXiv.org/format/astro-ph/0212177.

[5] Ipatov, S.I. and Mather, J.C.: Migration of small bodies and dust to near-Earth space, Advances in Space Research, Vol. 37, pp. 126-137, 2006. http://arXiv.org/format/astro-ph/0411004.

[6] Ipatov, S.I. and Mather, J.C.: Migration of comets to the terrestrial planets, Proceedings of IAU Symp. No. 236 "Near-Earth Objects, Our Celestial Neighbors: Opportunity and Risk". Cambridge: Cambridge Univ. Press, pp. 55-64, 2007. http://arXiv.org/format/astro-ph/0609721.

[7] Ipatov, S.I.: Collision probabilities of migrating small bodies and dust particles with planets, Proceedings of IAU Symposium S263. Vol. 5, "Icy bodies in the Solar System". Cambridge: Cambridge Univ. Press, pp. 41-44, 2010. http://arxiv.org/abs/0910.3017.

[8] Levison, H.F. and Duncan, M.J.: The long-term dynamical behavior of short-period comets, Icarus, Vol. 108, pp. 18-36, 1994.

[9] Marov, M.Ya. and Ipatov S.I.: Delivery of water and volatiles to the terrestrial planets and the Moon, Solar System Research, Vol. 52, N 5, in press, 2018.

EPSC Abstracts
Vol. 12, EPSC2018-532, 2018
European Planetary Science Congress 2018

Do magnetic fields modify tidal dissipation in the convective envelope of low-mass stars along their evolution?

Aurélie Astoul (1,2), Stéphane Mathis (1), Clément Baruteau (2), Antoine Strugarek (1), Emeline Bolmont (1), Florian Gallet (3), Kyle Augustson (1)
(1) Laboratoire AIM Paris-Saclay, CEA/DRF - CNRS - Univ. Paris Diderot - IRFU/DAp, Centre de Saclay, 91191, Gif-sur-Yvette Cedex, France; (2) IRAP, Université de Toulouse, CNRS, UPS, Toulouse, France; (3) Université Grenoble Alpes, CNRS, IPAG, 38000 Grenoble, France (aurélie.astoul@cea.fr)

Abstract

The dissipation of the kinetic energy of large-scale and wave-like tidal flows within the convective envelope of low-mass stars is one of the key physical mechanisms that shape the orbital and rotational dynamics of short-period exo-planetary systems. In the case of stable binary systems, they lead to the orbit circularisation and to the spins synchronisation and alignment; in the case of unstable systems they drive the spiraling of the planet towards the central star.

In addition, stellar convective envelopes are (differentially) rotating, turbulent, and magnetized regions where an active dynamo action is sustained (e.g. Brun & Browning 2017 and references therein). Therefore, as demonstrated by first theoretical works and numerical simulations, tidal flows and waves excitation, propagation, and dissipation can be impacted by stellar magnetic fields (e.g. Wei 2017, Lin & Ogilvie 2018, Wei 2018). For instance, the so-called dynamical tide is constituted of magneto-inertial waves (their restoring forces being the Lorentz force and the Coriolis acceleration) instead of inertial waves in the non-magnetized case. In the meanwhile, the amplitude and the geometry of dynamo-generated magnetic fields vary along the evolution of low-mass stars (e.g. Vidotto et al. 2014, Brun & Browning 2017 and references therein). In this framework, the key question that should be answered is "for which stellar masses, rotation and evolution phases, do we need to take into account the action of magnetic fields on tidal waves excitation, propagation, and dissipation?".

In this work, we identify the terms in MHD equations that should be computed to evaluate the impact of magnetic fields on tidal dissipation in the convective envelope of active rotating low-mass stars hosting planets. Using scaling laws that provide the amplitude of dynamo-generated magnetic fields along the structural and rotational evolution of these stars (e.g. Augustson, Mathis & Brun 2016) combined with detailed grids of rotating stellar models (e.g. Amard et al. 2016), we demonstrate that a full MHD treatment of tidal waves excitation, propagation, and dissipation is required for all low-mass stars (from M to F-type stars) all along their evolution. Consequences for the dynamical evolution of short-period exoplanetary systems are finally discussed.

Acknowledgements

A. A., S. M., E. B., and K. A. acknowledge funding by the European Research Council through ERC grant SPIRE 647383. F.G acknowledges financial support from CNES and the Swiss National Science Foundation (FNS) and from the SEFRI project C.140049 under COST Action TD 1308 Origins. This work was also supported by the Programme National de Planétologie (CNRS/INSU), the Programme National de Physique Stellaire PNPS (CNRS/INSU), and PLATO CNES grants at Départment d'Astrophysique (CEA-Saclay) and IRAP.

References

[1] Brun A.-S., Browning M. K., Living Reviews in Solar Physics, Vol. 14, 4, 2017.

[2] Wei X., The Astrophysical Journal, Vol. 828, 30, 2016.

[3] Lin Y., Ogilvie G., Monthly Notices of the Royal Astronomical Society, Vol. 474, p.1644-1656, 2018.

[4] Wei X., The Astrophysical Journal, Vol. 854, 34, 2018.

[5] Vidotto A., et al., Monthly Notices of the Royal Astronomical Society, Vol. 441, p. 2361-2374, 2014.

[6] Augustson K., Mathis S., Brun A.-S., The 19th Cambridge Workshop on Cool Stars, Stellar Systems, and the Sun (CS19) proceedings, 152, 2016.

[7] Amard, L., Palacios, A., Charbonnel, C., Gallet, F., Bouvier, J., Astronomy & Astrophysics, Vol. 587, 105, 2016.

EPSC Abstracts
Vol. 12, EPSC2018-608, 2018
European Planetary Science Congress 2018

Origin of close-in super-Earths: In-situ formation in an evolving disk due to disk winds

Masahiro Ogihara (1), Eiichiro Kokubo (1), Takeru K. Suzuki (2) and Alessandro Morbidelli (3)
(1) National Astronomical Observatory of Japan, Japan, (2) University of Tokyo, Japan, (3) Observatoire de la Côte d'Azur, France (masahiro.ogihara@nao.ac.jp)

Abstract

Observations of extrasolar planets have revealed a number of close-in super-Earths; however, their origin is still a matter of debate. We investigate the formation of close-in super-Earths in a protoplanetary disk that viscously evolves under the effects of magnetically driven disk winds by performing *N*-body simulations. We find that the type I migration is significantly suppressed because the gas surface density is decreased and has a flatter profile in the close-in region due to disk winds. When the type I migration is significantly suppressed, planets in a chain of mean-motion resonances undergo late orbital instability during the gas depletion, leading to a non-resonant configuration. In this case, observed distributions of close-in super-Earths (e.g., period ratio) can be reproduced by results of our simulations.

1. Introduction

Formation models of close-in super-Earths can be divided into two groups; namely, in-situ formation models and migration models. According to a recent study of in-situ formation of close-in super-Earths, planets grow and migrate very rapidly in a power-law disk based on the minimum mass solar nebula [1]. As a result, super-Earths form in a highly compact configuration near the disk inner edge, which is inconsistent with observed distributions.

Recent magnetohydrodynamic (MHD) simulations revealed the existence of magnetically driven disk winds [2, 3]. The global disk evolution including effects of disk winds was also investigated, which showed that disk profiles in the close-in region can be altered from a power-law distribution [4].

In this study, we perform *N*-body simulations of super-Earth formation from planetary embryos in a protoplanetary disk evolving with disk winds. Our main goal is to reproduce observed properties of close-in super-Earths by results of our *N*-body simulations.

2. Model

For evolution of disk surface density, we numerically solve the diffusion equation that includes effects of disk winds based on MHD simulations (the same as used by previous study [4]). As there exists uncertainties in the disk evolution model, we use several model parameters (e.g., turbulent viscosity). We find that when the turbulent viscosity is high ($\alpha \simeq 8\times10^{-3}$), the disk surface density obtains a flat profile in the close-in region (see the red line in Figure 1).

We start *N*-body simulations with planetary embryos of 0.2 Earth masses that are distributed in a ring-like region between 0.1 and 2 au from the central star. Orbital evolution is calculated by a fourth-order Hermite scheme with a hierarchical individual time step. For the formulae of type I migration, we use those described in a paper that takes into account the saturation of corotation torque [5].

3. Results

Figure 1 shows snapshots of the system for typical outcome of *N*-body simulations. Growth of planets proceeds from the inner region, and the mass of grown planets is larger than 1 Earth mass at $t > 0.1$ Myr. These planets should undergo rapid inward migration in the power-law disk model based on the minimum mass solar nebula; however the type I migration is significantly suppressed in a flat disk profile with effective desaturation of positive corotation torque. Most planets are in relatively close mean-motion resonances before the gas depletion, which are disrupted by orbital crossings during the gas dissipation phase (t > 1 Myr). In the final state, several close-in super-Earths form in a non-resonant configuration.

We perform a series of N-body simulations to statistically compare our results with observed distributions of close-in super-Earths. We find that the observed period-ratio distribution can be reproduced when planets do not undergo significant migration in a gas disk and resonant relationships are disrupted by orbital crossings during the disk dissipation phase. We also find that results of our N-body simulations are basically consistent with other observed characteristics (see also [6] for more details).

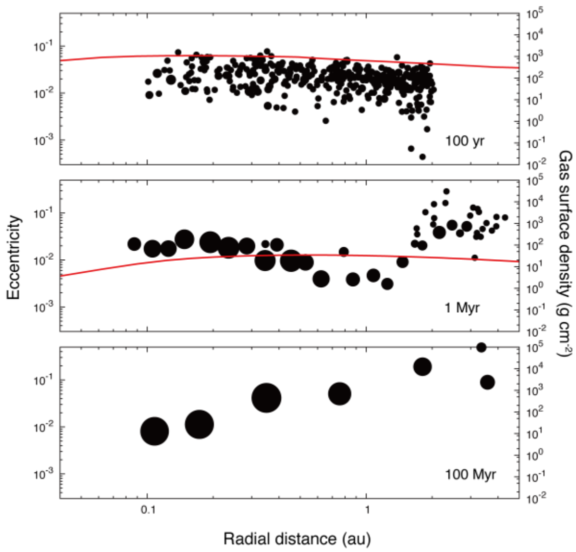

Figure 1: Snapshots of the system for our typical simulation. The filled circles represents the size of particles. The red lines indicate the gas surface density (right axis).

4. Summary and Conclusions

When the disk profile is altered due to the effect of disk winds, type I migration of super-Earth cores can be significantly suppressed. Slowly migrating planets are captured in mean-motion resonances. Such planets undergo late orbital instability during the gas dissipation phase, leading to a non-resonant configuration. In this case, observed distributions of close-in super-Earths (e.g., period ratio) can be reproduced.

Acknowledgements

This work was supported by JSPS KAKENHI Grant Numbers 16H07415 and 17H01105.

References

[1] Ogihara, M., Morbidelli, A., and Guillot, T.: A reassessment of the in situ formation of close-in super-Earths, *Astronomy & Astrophysics*, 578, A36, 2015.

[2] Suzuki, T. K., and Inutsuka, S.: Disk winds driven by magnetorotational instability and dispersal of protoplanetary disks, *The Astrophysical Journal*, 691, L49, 2009.

[3] Fromang, S., Latter, H., Lesur, G., and Ogilvie, G. I.: Local outflows from turbulent accretion disks, *Astronomy & Astrophysics*, 522, A71, 2013.

[4] Suzuki, T. K., Ogihara, M., Morbidelli, A., Crida, A., and Guillot, T.: Evolution of protoplanetary discs with magnetically driven disc winds, *Astronomy & Astrophysics*, 596, A74, 2016.

[5] Paardekooper, S. -J., Baruteau, C., and Kley, W.: A torque formula for non-isothermal Type I planetary migration – II. Effects of diffusion, *Monthly Notices of the Royal Astronomical Society*, 410, 293, 2011.

[6] Ogihara, M., Kokubo, E., Suzuki, T. K., and Morbidelli, A.: Formation of close-in super-Earths in evolving protoplanetary disks due to disk winds, *Astronomy & Astrophysics*, in press, 2018.

EPSC Abstracts
Vol. 12, EPSC2018-615, 2018
European Planetary Science Congress 2018

Geophysical Testing of Large Scale Migration of Planetesimals in the Early Solar System

Julie Castillo-Rogez (1) and Pierre Vernazza (2)

(1) Jet Propulsion Laboratory, California Institute of Technology, Pasadena, CA, USA, (2) Aix Marseilles Universite, CNRS, LAM, UMR 7326, Marseille, France.

Abstract

Per their large number, midsize asteroids in the 100-300 km diameter range represent the bulk of the mass of the asteroid belt after Ceres, Vesta, and Pallas are removed. This has been interpreted as a primordial feature [1], i.e., this generation of planetesimals accreted fast and then contributed to the growth of larger bodies. Smaller asteroids are fragments/debris from collisions between these midsize planetesimals, many of which are progenitors of asteroid families. Midsize planetesimals are also found in all small body reservoirs, such as the Kuiper Belt, the Trojan asteroids, and the irregular satellites. Phoebe stands out in the outer solar system as a high density planetesimal when most other 100-300 km objects in that region have cometary-like densities. Conversely, many asteroids found in the asteroid belt also have densities $\leq$1 g/cm^3. These discrepancies show that midsize planetesimals across the solar system had very different heat budgets and those currently found in the same reservoirs may have formed in different accretional environments.

1. Introduction

Comparison between populations of objects in the same size range can help constrain these environments via a quantification of the heat budget of these bodies, by taking current porosity estimates as a gauge of internal evolution. Gravitational energy and accretional heating are minor contributors to that class of bodies, per their small sizes. Heat from long-lived radioisotope decay cannot keep up with heat lost by diffusion from these small bodies. They might promote some creep-driven compaction depending on the volume fraction of volatiles, but otherwise these bodies are expected to remain globally porous. Only short-lived radioisotopes, and especially ^{26}Al, can incur dramatic internal changes, e.g., extensive compaction, ice melting, and then aqueous alteration. We know this to be the case for C*h* and C*gh* asteroids, the classes of C-type asteroids that display a water of hydration signature over their surfaces [2] and are believed to be parent bodies of the CI/CM chondrites [e.g., 3]. Hence the density and spectral properties of <300 km planetesimals provide first order constraint on the time of formation of these bodies. We track the evolution of porosity in these bodies in order to explain the disparities in porosity between main belt asteroids and irregular satellites, on the one hand, and Kuiper Belt objects and Trojan asteroids, on the other hand. We model the thermal and porosity evolution of midsize planetesimals based on previous work [4].

2. Genetic Relationships Between Reservoirs of Small Bodies

Similar evolution between Trojan asteroids, P- and D-type asteroids found in the main belt, Centaurs, and KBOs support a genetic relationship between these classes of bodies, as simulated by many studies [5]. Limited internal evolution is consistent with accretion models; for example [6] estimated that objects forming in the 20–25 AU region would take at least 5 My to start accreting and reach a 100 km radius in ~1 My.

Many irregular satellites display spectral properties akin to C-asteroids, such as Phoebe and Himalia. Saturn's satellite Phoebe was suggested to come from the Kuiper Belt based on the observation that its density matches the grain density inferred from cosmochemical models of bodies formed in the Solar nebula [4]. Thermal modeling showed that most of Phoebe's original porosity could be removed provided that it accreted in less than 4 My after calcium-aluminum inclusions taken as a time reference [4]. The density discrepancy between

Phoebe and KBO questions that relationship and cannot be uniquely explained by a difference in volatile content. Many previous studies noted the similarities between the spectra of Phoebe, Himalia, and hydrated asteroids and suggested that the two irregular satellites actually migrated from the inner Solar system [e.g., 7]. The Grand Tack and alternate models [8, 9] could provide an alternate scenario for a common origin for hydrated C-type asteroids and irregular satellites. In that context, the primary reservoir for C-types is between and beyond the orbits of the giant planets. So that material could have been available for capture by the giant planets early on. This model implies accretion was fast and early in that region, consistent with recent accretion scenarios [10]. Density and spectral variations found among the various subclasses of C-type asteroids might further support a scenario where these bodies formed at different distances from the Sun, i.e., between Jupiter-Saturn, Saturn-Uranus, and beyond, resulting in different volatile composition and heat budget.

3. Implications for Ceres

Following the logic introduced above, it might be possible to constrain the accretional environment of Ceres and Ceres-like asteroids (e.g., 10 Hygiea). Ammoniated material on Ceres' surface [11] and its large fraction of volatiles suggest that the dwarf planet formed from material originating beyond Jupiter. However, it is not confirmed yet whether Ceres as a whole originated far in the outer Solar system or if it grew from outer solar system planetesimals migrated to the main belt. It might be possible to constrain Ceres' time of formation assuming it formed in the same region of the solar system as 10 Hygiea, an asteroid that shares a similar surface composition involving carbonates and ammoniated clays [12]. Hygiea is half the size of Ceres and thus is more sensitive to the heat budget available post-accretion. Our modeling of Hygiea's thermal evolution requires ^{26}Al decay heat for its interior to reach conditions amenable for hydrothermal processing on a global scale. Furthermore, the depth of altered material should be relatively shallow in order to be exposed either by subcatastrophic disruption (which produced Hygiea's family) or by overturn of an unaltered crust. We infer a time of formation of less than 3.5 My after CAIs for Hygiea. This early formation is similar to that inferred for CM chondrite parent bodies [e.g., 13] and Phoebe [4].

4. Conclusion

The heat budget of midsize planetesimals varied across the Solar system. Jupiter Trojan asteroids, D/P asteroids in the main belt, and midsize KBOs appear to have preserved up to 40% bulk porosity, which we explain as accretion with few or no short-lived radioisotopes. This reinforces the genetic relationship between these classes of bodies proposed by dynamical models. On the other hand, C-type bodies distributed in the main belt and among the irregular satellite population show evidence for low-porosity and, in many cases, aqueously altered material on their surface. This suggests C-type bodies shared a common reservoir that possibly existed early on between the orbits of the giant planets [14].

Acknowledgements

A portion of this work was conducted by the Jet Propulsion Laboratory, California Institute of Technology, under contract with NASA.

References

[1] Cuzzi J. N. et al.: *Icarus* 208, 518-538, 2010.

[2] Rivkin, A. S. et al.: *Astron. J.* 150, id 198, 2015.

[3] Vernazza P. et al.: *Astron. J.* 152, 54, 2016.

[4] Castillo-Rogez J. et al.: *Icarus* 219, 86-109, 2012.

[5] Morbidelli A. et al.: *Nature* 435, 462-465, 2005.

[6] Kenyon S. J. et al. (2008) *In:* The Solar System Beyond Neptune, 293-312.

[7] Hartmann W. K. (1987) Icarus 71, 57-68.

[8] Walsh K. J. et al. (2011) *Nature* 475, 206-209.

[9] Raymond, S. N., Izodoro, A. (2017) *Icarus* 297, 134-148.

[10] Johansen A. et al. (2015) *Sci. Adv.* 2015;1:e1500109.

[11] De Sanctis M. C. et al. (2015) *Nature* 528, 241-244.

[12] Vernazza P. et al. (2017) *Astron. J.* 153, id. 72.

[13] Jogo K. et al. (2017) *Geochimica and Cosmochimica Acta* 199, 58-74.

EPSC Abstracts
Vol. 12, EPSC2018-879, 2018
European Planetary Science Congress 2018

Dynamical limitations on the habitability of planets in binary star systems

Ákos Bazsó and Elke Pilat-Lohinger
Institute for Astrophysics, University of Vienna, Austria (akos.bazso@univie.ac.at, elke.pilat-lohinger@univie.ac.at)

Abstract

Wide binary star systems with circumstellar exoplanets are generally believed to be conducive to habitable planets. We demonstrate that in the presence of a giant planet secular perturbations can affect the habitable zone (HZ) for a wide range of system parameters. Such perturbations lead to enhanced eccentricities of terrestrial planets and are detrimental to sustain habitable conditions on the planet. We develop a diagnostic tool based on analytical models that allows an easy identification of observed binary systems lacking habitable conditions from a dynamical point of view.

1. Introduction

Extrasolar planets have been detected in a great diversity of configurations. Especially, exoplanets are also present in binary and multiple star systems. The "Catalogue of Exoplanets in Binary Star Systems[1]" currently lists 125 planets in 88 different binary systems.

The habitability of a terrestrial planet is sensitive to its orbital eccentricity [7]. An increased eccentricity leads to strong variations in the insolation onto the planet, and thus to temperature fluctuations with large amplitudes. Secular perturbations from massive perturbers act to increase the planet's eccentricity. It has been shown that even wide binaries with stellar separations > 1000 au can cause an increase in planetary eccentricities which can lead to ejections [3].

Here, we focus on binary systems with circumstellar planets. We assume that there is a terrestrial planet in the HZ of the host star and a giant planet exterior to it, with a distant companion star (secondary) as a perturber. For such a configuration there always exist specific combinations of the secondary's orbital parameters that lead to enhanced perturbations in the HZ. The aim of our study is to identify these parameter combinations (depending on e.g. stellar masses, separation, eccentricity) for a wide variety of systems.

[1]http://www.univie.ac.at/adg/schwarz/multiple.html

2. Methods

The orbital precession frequencies of the planets are the key point in the dynamical description of the system. There already exists a semi-analytical method to determine these frequencies, see [6] and [2]. We extend this method and are now able to describe the dynamics by two coupled analytical models: the Andrade-Ines & Eggl [1] model and the Laplace-Lagrange model [5].

Since there is a multi-dimensional parameter space to cover, we focus on cases that are most relevant for habitable terrestrial planets. We vary the masses of both the host and secondary star; the choice of the host star's mass sets the location of the HZ [4]. We also take the secondary star's orbital distance and eccentricity as free parameters, which are generally poorly constrained from observations for wide binaries. Then, for a range of giant planet masses and distances, we can determine whether a secular perturbation would affect the HZ.

3. Results

The figure shows an example of a binary star system that consists of a G-type host star and an M-type secondary. The grey-shaded areas indicate combinations of the secondary star's orbital eccentricity and distance (as a function of the giant planet's fixed distance) for which the secular perturbation affects some part of the HZ. In such a case, a terrestrial planet in that part of the HZ would have an orbital precession frequency that corresponds to the one of the giant planet. The resonance between these two frequencies creates large scale variations of the terrestrial planet's orbital eccentricity, and hence limits its residence time inside the HZ.

As the figure demonstrates, even relatively far away secondary stars might push a terrestrial planet in the HZ to become eccentric. Depending on the actual orbital distance of the giant planet there always exist combinations of secondary star parameters that lead

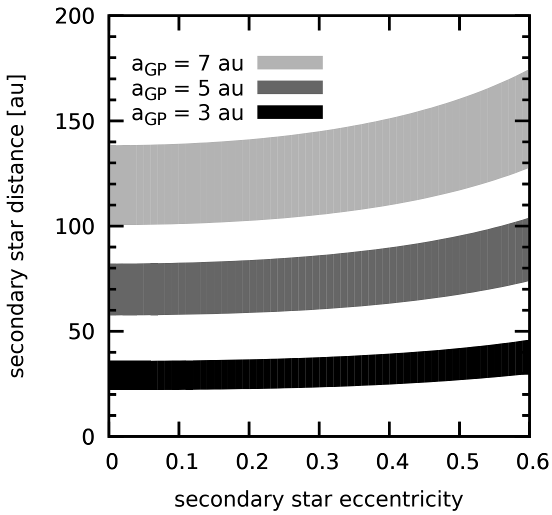

Figure 1: In a binary star system with a giant planet at different distances (see legend) a secular pertubation affects the habitable zone when the orbital parameters of the secondary star fall into the grey shaded areas.

to this kind of perturbations. For more distance giant planets the "zone of perturbations" becomes more extended than for close-in giants.

Apart from this one example, there are countless other configurations that could be realized. We are working to establish a catalogue that includes template systems, that can be used for a quick assessment of observed binary stars in the light of the findings above.

4. Conclusions

- In wide binary star systems with a giant planet, secular perturbations can affect the habitable zone for a wide range of orbital parameters of the secondary star.

- Due to the secular perturbation a terrestrial planet in the HZ would become more eccentric, which in turn increases the insolation onto the planet.

- Habitability over extended periods of times requires a limited variation in insolation, hence strong fluctuations in the eccentricity can severely limit the effective habitability of a planet.

Acknowledgements

This work was supported via the Austrian Science Fund (FWF) project S116-08 N16. The authors thank C. Lhotka, N. Georgakarakos, and Z. Knežević for useful discussions.

References

[1] Andrade-Ines, E. and Eggl, S.: Secular Orbit Evolution in Systems with a Strong External Perturber - A Simple and Accurate Model, AJ, Vol. 153, 148, 2017

[2] Bazsó, Á., Pilat-Lohinger, E., Eggl, S., Funk, B., Bancelin, D. and Rau, G.: Dynamics and habitability in circumstellar planetary systems of known binary stars, MNRAS, Vol. 466, pp. 1555-1566, 2017

[3] Kaib, N. A., Raymond, S. N. and Duncan, M.: Planetary system disruption by Galactic perturbations to wide binary stars, Nature, Vol. 493, pp. 381-384, 2013

[4] Kopparapu, R. K., Ramirez, R. M., SchottelKotte, J., Kasting, J. F., Domagal-Goldman, S. and Eymet, V.: Habitable Zones around Main-sequence Stars: Dependence on Planetary Mass, ApJL, Vol. 787, L29, 2014

[5] Murray, C. D. and Dermott, S. F.: Solar system dynamics, Cambridge University Press, 1999.

[6] Pilat-Lohinger, E., Bazsó, Á. and Funk, B.: A Quick Method to Identify Secular Resonances in Multi-planet Systems with a Binary Companion, AJ, Vol. 152, 139, 2016

[7] Williams, D. M. and Pollard, D.: Earth-like worlds on eccentric orbits: excursions beyond the habitable zone, International Journal of Astrobiology, Vol. 1, pp. 61-69, 2002

EPSC Abstracts
Vol. 12, EPSC2018-995, 2018
European Planetary Science Congress 2018

A survey of collision outcomes during planet formation: water transport and loss

Thomas I. Maindl (1), Philip M. Winter (1), Elke Pilat-Lohinger (1), Nader Haghighipour (2), Christoph M. Schäfer (3), Christoph Burger (1) and Rudolf Dvorak (1)

(1) Department of Astrophysics, University of Vienna, Austria, (thomas.maindl@univie.ac.at), (2) Institute of Astronomy and NASA Astrobiology Institute, University of Hawaii-Manoa, HI, USA, (3) Institut für Astronomie und Astrophysik, Eberhard Karls Universität Tübingen, Germany

Abstract

We present results of a suite of collision simulations covering a wide range of the involved objects' parameters such as mass, projectile-to-target mass ratio, material composition, collision velocity, and collision angle. These results will aid in estimating the amount of water retained and lost in dynamical planet formation studies.

1. Introduction

It is well-established that a long sequence of collisions of protoplanetary bodies was involved in forming terrestrial planets. In particular, it is widely accepted that water-carrying planetary embryos and planetesimals from beyond the snowline – maybe even comets ([5]) – delivered a large fraction of Earth's water. Most existing planet formation studies treat those collisions as perfect inelastic merging events (e.g., [4, 6]) or apply simple fragmentation models ([1]) hereby ignoring the actual collision outcome in terms of fragmentation and water loss. As a consequence, these planet formation simulations overestimate the water content of the formed terrestrial planets – estimates range from about 30 % less water being transported to the habitable zone ([2]) to a factor of 5-10 ([3]).

2. Simulations and results

To aid the efforts of more accurately estimating the actual water transport rates to the habitable zone, we performed a number of collision simulations with our parallel 3D smooth particle hydrodynamics (SPH) code ([8, 9]) in the past (e.g., [7, 2]). The preliminary results in Figure 1 show the water loss (color-coded) after collisions of Ceres-mass objects at different collision velocities (measured in units of the mutual escape velocity) and angles (0° corresponds to a head-on collision). Note that for collision angles ≳40° (hit-and-run collisions), the water loss is significantly lower than for eroding collisions at smaller angles and high velocity.

In order to study how the water loss additionally depends on the involved masses, projectile-to-target mass ratios, and water contents, we will present new results from a suite of several hundred collision simulations with varying parameters.

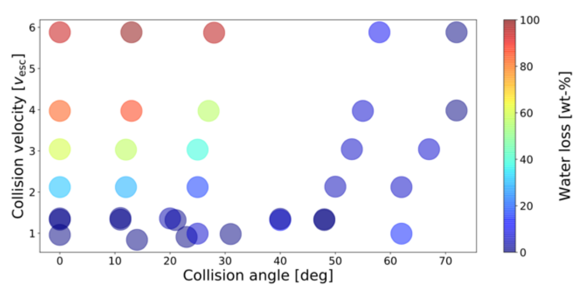

Figure 1: Water loss (color-coded) after collisions of Ceres-size objects with 30 wt-% water mass fraction. Results from SPH-simulations.

Acknowledgements

TIM, PMW, CB, and RD acknowledge support from the FWF Austrian Science Fund project S11603-N16, EPL from project S11608-N16. NH acknowledges support from the NASA PAST program under grant NNX14AJ38G.

References

[1] S. G. Alexander and C. B. Agnor. *Icarus*, 132, 113-124, 1998.

[2] D. Bancelin, E. Pilat-Lohinger, T. I. Maindl, F. Ragossnig, and C. Schäfer. *AJ*, 153, 269, 2017.

[3] N. Haghighipour and S. N. Raymond. *ApJ*, 666, 436-446, 2007.

[4] A. Izidoro, K. de Souza Torres, O. C. Winter, and N. Haghighipour. *ApJ*, 767, 54, 2013.

[5] B. Loibnegger, R. Dvorak, M. Cuntz. *AJ*, 153, 203, 2017.

[6] J. I. Lunine, D. P. O'brien, S. N. Raymond, A. Morbidelli, T. Quinn, and A. L. Graps. *Advanced Science Letters*, 4, 325-338, 2011.

[7] T. I. Maindl, R. Dvorak, C. Schäfer, and R. Speith. *IAU Symposium*, 310, 138-141, 2014.

[8] T. I. Maindl, C. Schäfer, R. Speith, Á. Süli, E. Forgács-Daika, and R. Dvorak. *AN*, 334(9), 996-999, 2013.

[9] C. Schäfer, S. Rieker, T. I. Maindl, R. Speith, S. Scherrer, and W. Kley. *A&A*, 590, A19, 2016.

EPSC Abstracts
Vol. 12, EPSC2018-1010, 2018
European Planetary Science Congress 2018

Relaxation of resonant two-planet systems and their TTVs

Rosemary Mardling (1,2)
(1) School of Physics and Astronomy, Monash University, (2) Astronomy Department, University of Geneva
(rosemary.mardling@monash.edu)

Abstract

Many two-planet systems reside near or inside first-order resonances. These are normally the product of planet-disk interactions during the time of formation, with eccentricity damping and migration resulting in a relaxed system with fewer degrees of freedom than for an arbitrary two-planet system. We will present a simple formulation describing such systems which is valid inside, across and outside the resonance. We will show that all such systems are governed by a single two-parameter ordinary integro-differential equation, and that all system information (variation of eccentricities, orbital frequencies, resonance angles, apsidal orientations, transit timing variations or TTVs) can be derived from its solution. The expression for the TTVs can be easily inverted to solve for the planet masses (and other system parameters) when both planets transit; if no valid inversion is possible (given sufficient signal to noise for the TTVs), it is possible to infer the existence of non-transiting planets, the signature of which will be imprinted on the signal.

EPSC Abstracts
Vol. 12, EPSC2018-1021-1, 2018
European Planetary Science Congress 2018

Enrichment of Heavy Elements in Gas Giant Planets during the Supply-Limited Accretion Phase

Sho Shibata , Masahiro Ikoma
Earth and Planetary Science, School of Science, University of Tokyo
(s.shibata@eps.s.u-tokyo.ac.jp)

Abstract

Recent studies of internal structure of gas giants suggest that their envelope is enriched with heavier elements than hydrogen and helium, relative to their central star composition. Previous studies examined the possibility of additional increase of heavy elements through the capture of planetesimals in the vicinity of a growing protoplanet in constant protoplanetary disk. However, it is well known that sufficiently massive protoplanet opens a gap in the protoplanetary disk(PPD) and circumplanetary disk(CPD) is formed around it. Gap structure would change the growth rate of protoplanet and accretion rate of planetesimals, and CPD also change the accretion rate. In this study, we investigated the effects of opening of gap in PPD and formation of CPD on the accretion rate of planetesimals. We find that both of the opening of gap structure in PPD and formation of CPD enhance the accretion rate.

1. Introduction

Recent studies suggest that gas giants' envelope is enriched with heavier elements. It is considered that these enrichment in heavy elements are caused by the capture of planetesimals during the late formation stage of gas giant. Zhou & Lin 2007 and Shiraishi & Ida 2008 performed orbital integration of planetesimals around growing protoplanet in constant protoplanetary disk, and Shiraishi & Ida estimated the total captured mass of planetesimals for Jupiter and Saturn. However, their simplified constant disk model might be incorrect, because it is well known that sufficiently massive protoplanet opens a gap in the protoplanetary disk(PPD) and circumplanetary disk(CPD) is formed around it. Gap structure would change the growth rate of protoplanet and accretion rate of planetesimals, and CPD would also change the accretion rate. In order to estimate the total captured mass of planetesimals through protoplanet growth, these effects have to be evaluated correctly.

2. Aims of Study

A system composed with a central star, a massive protoplanet and negligibly small planetesimals can be treated as a restricted three body problem. In this system, planetesimals conserve Jacobi energies $E_{\rm Jacobi}$ which is written as

$$E_{\rm Jacobi} \equiv \frac{1}{2}v'^2 + U_{\rm Jacobi}, \quad (1)$$

where v' is a velocity of planetesimals on the corotating flame and $U_{\rm Jacobi}$ is Jacobi potential written as

$$U_{\rm Jacobi} = -\mathbf{h}\cdot\mathbf{n}_{\rm p} - G\frac{M_{\rm s}}{r_{\rm pl,s}} - G\frac{M_{\rm p}}{r_{\rm pl,p}}, \quad (2)$$

where $\mathbf{h}$, $\mathbf{n}_{\rm p}$ are angular momentum of planetesimal and mean motion of protoplanet. $M_{\rm s}$ and $M_{\rm p}$ are mass of central star and protoplanet, and $r_{\rm pl,s}$ and $r_{\rm pl,p}$ are relative distance between planetesimal and central star, and between planetesimal and protoplanet, respectively.

The capture process of planetesimals is divided into two stages. First stage is the entering into the feeding zone. In order to enter the Hill Sphere of protoplanet, planetesimals have to flow over the potential barrier surrounding the protoplanet. The area which meets this requirement condition is called as feeding zone, and defined as

$$E_{\rm Jacobi} > 0. \quad (3)$$

Thus, planetesimals' Jacobi energy have to be increased in this stage. Second stage is the capture by the Hill Sphere. In order to be captured by the protoplanet gravitaionally, planetesimals have to lose their escape energy in the Hill Sphere.

The change of the Jacobi energy occurs due to the increase of protoplanet mass and the drag of disk gas. Thus, we expect that the capture process of planetesimals is closely tied to the disk gas structure. In this study, we construct the gap opened disk model and CPD formed disk model. Performing the orbital integration of planetesimals around growing protoplanet in these models, we get the total captured mass of planetesimals in each models. Comparing the results with those performed in the constant disk model, we evaluate the enhancement rate of captured mass due to the gap opening and circumplanetary disk formation, respectively.

3. Results

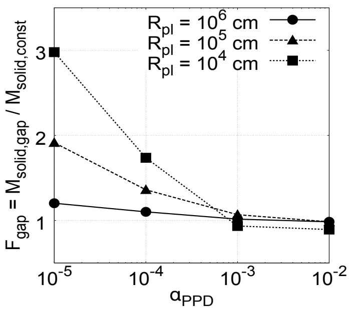

Figure 1: The change of the enhancement rate due to the gap opening with the viscosity of protoplanetary disk. The enhancement rate is defined in eq. 4. The solid, dashed and dotted lines show the case of $R_{\rm pl}{}^6$cm, $R_{\rm pl}{}^5$cm and $R_{\rm pl}{}^4$cm, respectively. The enhancement factor increases with the size of planetesimals and the width and depth of gap (gap is wider and deeper for small disk viscosity). These results suggests that the opening of gap changes the inflow flux of planetesimals into the feeding zone.

We define the enhancement rate of captured mass due to the gap opening in PPD as

$$f_{\rm gap} \equiv \frac{M_{\rm solid,gap}}{M_{\rm solid,const}}, \quad (4)$$

where $M_{\rm solid,gap}$ and $M_{\rm solid,const}$ are total captured mass of planetesimals in the gap opened disk model and constant disk model, respectively. Investigating the detailed effects of the gap opening, we performed the parameter study for the size of planetesimals $R_{\rm pl}$ and the disk viscosity $\alpha_{\rm PPD}$. Fig 1 shows the result of numerical calculations. Gap is wider and deeper for small disk viscosity, so the enhancement factor increases with the size of planetesimals and the width

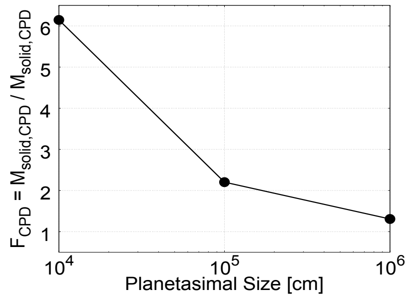

Figure 2: The change of the enhancement rate due to the formation of CPD with the size of planetesimals. The enhancement rate is defined in eq. 5. The enhancement factor is larger for smaller planetesimals, and this is because strong gas drag in Hill Sphere increases the capture probability.

and depth of gap. These results suggest that gap opening change the inflow flux of planetesimals into the feeding zone, namely first stage of planetesimal capture process.

We also define the enhancement rate of captured mass due to the formation of CPD as

$$f_{\rm CPD} \equiv \frac{M_{\rm solid,CPD}}{M_{\rm solid,const}}, \quad (5)$$

where $M_{\rm solid,CPD}$ is total captured mass of planetesimals in the CPD formed disk model. Investigating the detailed effects of the formation of CPD, we performed the parameter study for the size of planetesimals $R_{\rm pl}$. Fig 2 shows the result of numerical calculation. The enhancement factor is larger for smaller planetesimals. The formation of CPD changes the gas structure in the Hill Sphere, so it increases the losing rate of Jacobi energy in Hill Sphere and affect the second stage of planetesimal capture process. The losing rate of Jacobi energy is larger for smaller planetesimals, which consistent with our results.

References

[1] Zhou J.-L., Lin D. N. C., 2007, apj, 666, 447

[2] Shiraishi M., Ida S., 2008, apj, 684, 1416

EPSC Abstracts
Vol. 12, EPSC2018-1046, 2018
European Planetary Science Congress 2018

Dynamical perturbations of Earth-type planets in binary star systems

Elke Pilat-Lohinger (1), Ákos Bazsó (1) and Nader Haghighipour (2)
(1) Department of Astrophysics, University of Vienna, Austria, (2) Institute of Astronomy, University of Hawaii-Manoa, (elke.pilat-lohinger@univie.ac.at, akos.bazso@univie.ac.at, naderh@hawaii.edu)

Abstract

In this study, we investigate gravitational perturbations (i.e. mean motion resonances MMR and secular resonances SR) on an Earth-type planet moving in the habitable zone which are caused by a Jupiter-Saturn pair and a distant secondary star. While MMRs can be easily determined via a simple formula SRs need a more sophisticated technique for their determination. However, in a binary system the location of such a perturbation can be determined in a simpler way, namely with the aid of a semi-analytical method which has been developed recently [1], [2]. As an example we show the results for a "G-M" binary star system (i.e. a G-type host-star and an M-type secondary star) for which we consider a stellar distance of 50 au and study different locations of the Jupiter-Saturn pair.

1. Introduction

After two decades of exo-planetary research our Earth is still the only habitable planet we know, which leads to the question whether solar system-like configuration need to be discovered to find an exo-Earth. In addition, many stars in the solar neighborhood form binary or multiple star systems which motivated us to study the gravitational perturbations in the circumstellar habitable zone (HZ) of a "G-M" binary star system where the G-type star hosts three planets: a Jupiter-Saturn pair and a terrestrial planet in the habitable zone, and the M-type star is the perturbing secondary. Considering a stellar separation of 50 au, one can calculate the locations of gravitational perturbations in the area of the terrestrial planet. Depending on the location of the gas planets Jupiter and Saturn we have determined the positions for the arising SRs between ~0.3 and 1.9 au, where some SRs can be found inside the HZ. In case the positions of the SR and the terrestrial planet are equal, the SR might cause an increase in the orbital eccentricity of the terrestrial planet. As a consequence the conditions for habitability will change for this planet so that stronger variations in the insolation arise (as discussed in [3])

2. Semi-analytical method

With the aid of the well-known Laplace-Lagrange secular perturbation theory (see e.g. [4]) one can derive an analytical solution for the proper frequencies of test-planets moving in a certain area – in our case between 0.1 and 2 au. To apply this theory we have to consider nearly zero eccentricities and inclinations for these orbits.

For the giant planets we compute the orbital motion and use a frequency analysis [5] to determine their proper frequencies. In case a frequency of a giant planet equals that of a test-planet an SR occurs.

3. Results

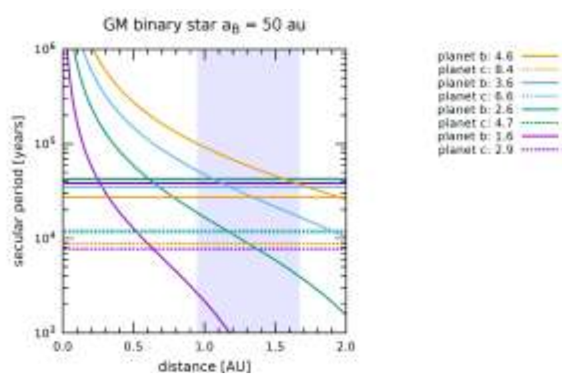

Figure 1: Location of the SR for different Jupiter (= planet b) - Saturn (= planet c) configurations. The blue vertical band marks the HZ.

The application of the semi-analytical method to various Jupiter-Saturn configurations in a binary star system with stellar separation of 50 au is shown in

Figure 1. In this figure, Jupiter is labeled as planet b (full lines) and Saturn as planet c (dashed lines). All Jupiter-Saturn configurations are in 5:2 MMR like in the solar system but closer to the G-type host-star as indicated in the legend to the right of the figure. We moved the two planets towards the host-star due to stability reasons caused by the perturbing secondary star.

The locations of the SRs are defined by crossings of a horizontal line (which define the proper period of the giant planets) with a curve (i.e. proper period of test-planets) of the same color. This result shows that only two planets cause SRs in the HZ. Which is the case if Jupiter's semi-major axis is 3.6 au and if Saturn's semi-major axis is 4.7 au. In all other cases the SRs are outside the HZ.

A more detailed study (of various masses and semi-major axes of the secondary star) is in progress and will be published soon.

Acknowledgements

EPL and BA want to acknowledge the Austrian Science Fund (FWF) for the financial support of this work which was carried out in the framework of the projects P22603-N16 and S11608-N16 – a subproject of the NFN Project "Pathways to Habitability". NH acknowledges support from the NASA PAST program under grant NNX14AJ38G.

References

[1] Pilat-Lohinger, E, Bazsó Á. and Funk, B: AJ, 152, 139, 2016.

[2] Bazsó, Á., Pilat-Lohinger, E., Eggl, S., Funk, B., Bancelin, D. and Rau, G.: MNRAS, 466, 1555, 2017.

[3] Williams, D.M and Pollard D.: IJAS, 1, 61, 2002

[4] Murray, C.D., Dermott, S.R: Solar System Dynamics, Cambridge University Press, 1999

[5] Regen, P.: A&A, 467, 1353, 2007

EPSC Abstracts
Vol. 12, EPSC2018-1070, 2018
European Planetary Science Congress 2018

Early tidal evolution of the TRAPPIST-1 system

Emeline Bolmont (1), Gavin Coleman (2), and Sergi Blanco-Cuaresma (3)
(1) Laboratoire AIM Paris-Saclay, CEA/Irfu Université Paris Diderot CNRS/INSU, Gif-sur-Yvette, France (emeline.bolmont@cea.fr) (2) University of Bern, Center for Space and Habitability, Gesellschaftsstrasse 6, CH-3012 Bern, Switzerland (3) Harvard-Smithsonian Center for Astrophysics, 60 Garden Street, Cambridge, MA 02138, USA

Abstract

Detection of planetary systems around ultracool dwarfs (i.e., stars with effective temperatures lower than 2 700 K) are expected to increase in the coming years [1] thanks to on-going efforts such as the TRAPPIST survey and future missions such as the project SPECULOOS. These systems can have several planets in compact orbital configurations, and they can be in or close to mean motion resonances as already observed in TRAPPIST-1 [2]. Planets arranged in this kind of set-up are surely affected by tidal effects, and the use of N-body simulation is necessary to understand both the formation and the consequent evolution of the system.

1. Introduction

In the lifetime of a system, the physical parameters governing star-planet interactions evolve quite significantly. Indeed, both stellar radius and rotation evolve during the pre-main sequence, which can last up to a few Gyr for ultracool dwarfs. In particular, this means that after the protoplanetary disk dispersal (at an age of a few Myr) due to a large stellar radius, the tide raised by the planets on the star, i.e. the stellar tide, was much stronger than today.

The dynamics governing the young TRAPPIST-1 system was therefore different than that of today. We aim at investigating these early phases of the evolution of TRAPPIST-1 to understand how the resonant chain came to evolve as what we see today.

2. Initial conditions: migration and formation within the disk

The initial conditions for the tidal simulations are outputs from planet formation models of planets embedded in the protoplanetary disk. We use two kinds of simulations for the earliest phases of the system. The first set of simulations initially took into account 29 already formed planetary embryos of 0.2 $M_\oplus$, which collided with one another and migrated in the disk. The second set of simulations reproduces more accurately the growth of the planets from small embryos through either pebble or planetesimal accretion [3].

These simulations end with the protoplanetary disk dispersal (at an age of 4 Myr) with chains of planets in resonance. However, the resonance of the inner pair is quite different to what is observed today: the simulations lead to a 3:2 resonance while the observations show a 8:5 resonance [2].

3. Tidal evolution model: post-disk evolution

In order to see if the resonances can change through tides during the early phase of the system, we use Posidonius [4]. It is a N-body code which takes into account both stellar tide and planetary tide, but also the evolution of the radius of the star [5] and its spin (accounting for contraction and stellar winds). We assume an initial stellar of spin of 2 days at an age of 4 Myr and use stellar wind parameters that allow to reproduce the $\sim$3 day spin observed today [6].

We explore several dissipation factors for the star and planets to account for the uncertainties we have on these parameters to investigate the rich dynamics of the system and also investigate how the planetary resonant chains evolve with time.

Acknowledgements

E.B. acknowledges funding by the European Research Council through ERC grant SPIRE 647383.

References

[1] Gillon, M., and 14 colleagues: Temperate Earth-sized planets transiting a nearby ultracool dwarf star, Nature, Vol. 533, pp. 221, 2016.

[2] Gillon, M., and 29 colleagues: Seven temperate terrestrial planets around the nearby ultracool dwarf star TRAPPIST-1, Nature, Vol. 542, pp. 456, 2017.

[3] Coleman, G., and colleagues, in prep.

[4] Blanco-Cuaresma, S., Bolmont, E.: Studying Tidal Effects In Planetary Systems With Posidonius. A N-Body Simulator Written In Rust, EWASS Special Session 4 (2017): Star-planet Interactions, 2017.

[5] Baraffe, I., Homeier, D., Allard, F., Chabrier, G.: New evolutionary models for pre-main sequence and main sequence low-mass stars down to the hydrogen-burning limit, Astronomy and Astrophysics, Vol. 577, pp. A42, 2015.

[6] Luger, R., and 32 colleagues: A seven-planet resonant chain in TRAPPIST-1, Nature Astronomy, Vol. 1, pp. 129, 2017.

EPSC Abstracts
Vol. 12, EPSC2018-1122-2, 2018
European Planetary Science Congress 2018

Second-order mean-motion resonances in a system of two low-mass planets

Zijia Cui (1), John Papaloizou (2) and Ewa Szuszkiewicz (1)
(1) Faculty of Mathematics and Physics and CASA*, University of Szczecin, Poland, (2) DAMTP, University of Cambridge, UK

Abstract

It is well known that first-order mean-motion resonances are common outcomes of the con- vergent orbital migration of low-mass planets in gaseous protoplanetary discs (Papaloizou and Szuszkiewicz, 2005). The attainment and maintenance of these resonances by migrating planets in the terrestrial mass range have been extensively studied by means of hydrody- namic simulations, simple analytic modelling and N-body investigations. The number of planetary systems in which the period ratios are close to a commensurability is increasing thanks to an ongoing intensive search for planets from the ground and space. However, among the observed period ratios one can find not only the first-order commensurabilities but also those of the second-order, like for instance 5:3, 7:5 or 9:7. The latter are of course less numerous than first order resonances but for sure not less intriguing. Are such resonant configurations easily induced by orbital migration? What are the conditions occurring in the protoplanetary disk which favour their formation? With these questions in mind we explore the attainment of the 9:7 resonance in a system which con- tains a pair of migrating low-mass planets. We have performed a series of hydrodynamical simulations with a variety of different initial disc parameters and planet mass ratios. We con- clude from our investigations that the resonance capture is possible if the relative convergent migration is slow and the planets have moderate eccentricities. We have compared our results with the simple analytic theory presented in the paper of Xiang-Gruess and Papaloizou (2015) which provides the conditions for the formation of the second order commensurabilities. It has been found that these conditions are consistent with our simulations. Moreover, our results are also accordant with the general model of resonance capture discussed in Mustill and Wyatt (2011).

Acknowledgements

The work has been supported by the Polish National Science Centre MAESTRO grant DEC-2012/06/A/00276. Numerical computations have been carried out on the HCP Hal9000 at the Faculty of Mathematics and Physics, University of Szczecin, Poland

References

[1] Mustill, Alexander J.; Wyatt, Mark C. (2011), MNRAS 413, 554

[2] Papaloizou, J. C. B.; Szuszkiewicz, E. (2005), MNRAS 363, 153

[3] Xiang-Gruess, M.; Papaloizou, J. C. B. (2015), MNRAS 449, 3043

EPSC Abstracts
Vol. 12, EPSC2018-1128, 2018
European Planetary Science Congress 2018

Improved encounter scenario for planetary embryos – A comparison between single-star and binary-star systems

Elke Pilat-Lohinger (1), Thomas I. Maindl (1), David Bancelin (1), Christoph Schäfer (2), Ákos Bazso (1)
(1) Department of Astrophysics, University of Vienna, Austria, (2) Eberhard Karls Universität Tübingen, Tübingen Germany, (elke.pilat-lohinger@univie.ac.at)

Abstract

For terrestrial planet formation the so-called perfect merging is commonly used even if this assumption is a weak point in the formation scenario. Including results from simulations of real collisions using SPH (Smooth Particle Hydrodynamics) provide better results for the growth of planetary embryos and lead therefore to a more realistic formation scenario. The improvements due to SPH simulations will be figured out for single and binary star systems as part for comparison.

1. Introduction

The growth of terrestrial planets from proto-planetary embryos is usually simulated with the aid of perfect merging without considering fragmentation so that two bodies merge completely once their mutual distance becomes smaller than a pre-defined collision threshold. The consideration of fragmentation in different collision outcome regimes as suggested by [1] is a first step to a more sophisticated model. Recently [2] showed the strong influence of fragmentation of and water-loss from small bodies on the final outcome of impacts in the context of a water-transport-study in binary star systems.

We therefore continue this study and present in a similar way a more realistic formation scenario which includes SPH-simulations of collisions. Such simulations provide information about volatile and material loss during impact which improves the simple hit and stick scenario.

In this context, we study collisions of Moon and Mars sized objects which obit the sun in the habitable zone (HZ) – i.e. between 0.95 and 1.7 au according to [3]. These proto-planetary embryos are perturbed by a Jupiter-mass planet at 3 au and a secondary star with distances between 25 and 100 au from the host-star. The system configuration influences the impact velocity and angle which quantifies the mass-loss during a collision. Moreover, as indicated already in [2], this study reveals also a significant increase in the encounter velocity in binary stars in contrast to single stars.

2. Computations

Part I: N-body simulation of a circumstellar disk of planetesimals and proto-planetary embryos have been performed in a binary star system of two Sun-like stars with a stellar separation of 50 au and an eccentricity of 0.3. Additional perturbations are caused by a Jupiter-like planet orbiting the host-star at about 3 au. For the embryos we took Moon- and Mars-size bodies.

Part II: Detailed simulations of water-rich Ceres-sized asteroids with dry target bodies of a Moon or Mars mass using a 3D SPH code [4], [5]. For the collision scenario 500,000 SPH particles are used in general (only in some cases this number was increased to more than 1 million SPH particles). The key parameters for the SPH collisions are the impact angles and impact velocities of the planetesimals.

Part III: Combining the results of Part I and Part II lead to more realistic values for the growth of bodies and water transport.

3. Results

An example for this 3-step scenario is shown in figure 1 where we compare a pure N-body simulation assuming perfect merging (black dashed line) with our proposed 3-step procedure (blue line). The two lines indicate significant modifications in the result when fragmentation and water-loss is taken into account (blue line). This sample plot shows the amount of water transported to terrestrial planets in the HZ via Ceres-sized planetesimals. Especially, in case of strong gravitational perturbations (i.e. resonances) which cause a higher eccentricity of the planetary motion, the assumption of perfect merging will overestimate the growth and water transport to a planet as it has been pointed out already in [2]. This difference is caused by higher impact velocities which lead to a higher water-loss.

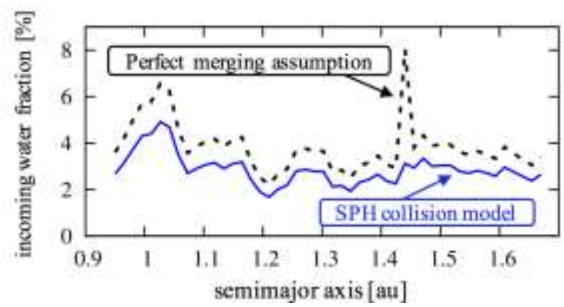

Figure 1: The water fraction transported via planetesimals onto a planet moving in the HZ when perfect merging is assumed (black dashed line) and when fragmentation and water-loss is taken into account (blue line).

Comparing the impact velocities of planetesimals and embryos in single and binary star systems, we recognized significantly higher impact velocities in binary stars. A more detailed study thereto is in progress and will be published soon.

Acknowledgements

The authors want to acknowledge the Austrian Science Fund (FWF) for the financial support of this work which was carried out in the framework of the projects S11608-N16 (EPL, DB and AB) and S11603-N16 (TIM) – subprojects of the NFN Project "Pathways to Habitability".

References

[1] Leinhardt, Z.M. and Stewart, S.T., ApJ, 745, 79, 2012

[2] Bancelin, D., Pilat-Lohinger, E., Maindl, T.I. et al., AJ, 153, 269, 2017

[3] Kopparapu, R.D., Ramirez, R.M., SchottelKotte, J., Kasting, J. et al., APJL, 787, L29, 2014

[4] Maindl, T.I, Schäfer, C., Speith, R. et al., AN, 334, 996, 2013

[5] Schäfer, Ch., Riecker, S., Maindl, T.I. et al., A&A 590, A19, 2016